Continental Shelf Research 277 (2024) 105253

Contents lists available at ScienceDirect

Continental Shelf Research

journal homepage: www.elsevier.com/locate/csr

Environmental controls on the interannual variability in chlorophyll and phytoplankton community structure within the seasonal sub surface chlorophyll maximum in the western English channel

Michelle L. Barnett, Alan E.S. Kemp, Anna E. Hickman, Duncan A. Purdie *

School of Ocean and Earth Science, National Oceanography Centre Southampton, University of Southampton Waterfront Campus, European Way, Southampton, SO14 3ZH, United Kingdom

ARTICLE INFO

Keywords:
Western English Channel
Subsurface chlorophyll maximum
Thermocline stratification
Phytoplankton community structure
Turbulence

ABSTRACT

The subsurface chlorophyll maximum (SCM) is increasingly recognised as an important but understudied locus of primary production particularly in shelf seas. Here we report the results of a 4 year, repeat station, summer sampling programme (2013–2016) of a seasonally recurrent SCM in the Western English Channel. Interannual variability in phytoplankton community structure and chlorophyll distribution and intensity was strongly related to water column stability at the depth interval of the SCM and also to water temperature. The phytoplankton community was statistically distinct in each year. High stability, as evidenced by large Richardson numbers and a well-developed strong thermocline appeared to favour the growth of larger dinoflagellates (autotrophs or mixotrophs) and diatoms. Such conditions led to development of the most intense SCMs and these were sometimes dominated by a single or a few key species most prominently in 2015 with near monospecific concentrations of the dinoflagellate *Tripos fusus* with average peak SCM chlorophyll concentrations of 7.3 ± 4.4 μg l^{-1}. By contrast, in years with low water column stability and intermittent turbulence at the thermocline (2014, 2016) there was greater chlorophyll dispersal and less intense SCM. In these low stability conditions, red fluorescent nanophytoplankton, such as naked dinoflagellates, chlorophytes and prymnesiophytes, made a greater contribution to the community, possibly as a result of the advantages that motility and enhanced light utilisation efficiency confer within an SCM exposed to turbulence. It is also likely that turbulence disrupted the stability required by the larger dinoflagellates and diatoms. Several of the key SCM taxa were absent from surface waters including the dinoflagellates *Tripos fusus*, *Tripos lineatus*, and most of the *Rhizosolenia/Proboscia* diatoms, consistent with adaptations more suited to survival at depth in stratified waters. These traits include luxury nutrient uptake and storage and survival in low light (both groups) and mixotrophy (dinoflagellates). On the other hand, in 2013, diatoms including *Pseudo-nitzschia* spp. were abundant in both surface, SCM and bottom waters. The relatively cooler waters (11.6–12.1 °C on average in 2013 and 2016) were characterised by smaller diatoms (*Chaetoceros* spp. and *Pseudo-nitzschia spp.*) whereas the warmer waters (13.1 °C on average in 2014) contained larger diatoms (large *Rhizosolenia* spp., *Lauderia annulata* and *Leptocylindrus danicus*). There did not appear to be continuity of key species between years, other than for the dinoflagellate *Tripos lineatus*, which was significant in both 2013 and 2014 and present in 2015. In any given year, there was no correspondence between the key spring bloom phytoplankton species as monitored in the nearby Western Channel Observatory L4 station and the key SCM taxa.

1. Introduction

Marine phytoplankton undertake around half of global photosynthesis, form the base of the ocean's food chains and, via the marine biological carbon pump, draw down atmospheric CO_2. The phytoplankton of shelf seas (<500 m water depth) are of particular importance, since they contribute ~ 15–30% of all oceanic primary production and despite their relatively small surface area (~8% of global total) are responsible for ~ 47% of the global annual export of particulate organic carbon (Jahnke, 2010; Wollast, 1998). Shelf sea

* Corresponding author.
E-mail address: dap@soton.ac.uk (D.A. Purdie).

https://doi.org/10.1016/j.csr.2024.105253
Received 5 January 2024; Received in revised form 11 May 2024; Accepted 13 May 2024
Available online 16 May 2024

phytoplankton are also the base of food chains that support over 90% of global fish catches (Pauly et al., 2002). Understanding the impacts of climate change on shelf sea phytoplankton community structure is therefore of critical importance in order to predict the consequences for the carbon cycle and for fisheries. Moreover, shelf seas are particularly sensitive to climatic variation (Backhaus, 1996; Holt et al., 2010, 2016; Sharples et al., 2006), which given their ecological and biogeochemical significance, makes knowledge of shelf sea phytoplankton and their response to environmental variation especially valuable.

Within seasonally stratified waters of high latitude and temperate shelf seas, considerable phytoplankton biomass is represented by the subsurface chlorophyll maximum (SCM) associated with the seasonal pycnocline (Cullen, 1982, 2015; Hickman et al., 2012; Holligan et al., 1984a; Holligan and Harbour, 1977; Martin et al., 2010; Pingree et al., 1978; Weston et al., 2005). These subsurface features have often been observed with maximum chlorophyll concentrations greater than 4 μg l^{-1} (Holligan et al., 1984a, 1984b; Lips et al., 2010; Martin et al., 2010; Richardson et al., 2000) and in some cases greater than 40 μg l^{-1} (Sharples et al., 2001; Sullivan et al., 2010), and can be sustained for periods of months as stratification persists. The SCM is a key site of carbon fixation, and has been estimated to contribute on average, approximately 35 - ≥ 65 % of summer primary production (Hickman et al., 2012; Martin et al., 2013; Richardson et al., 1998; Weston et al., 2005) and their total annual contribution is of the same order as (Fernand et al., 2013; Hickman et al., 2012; Williams et al., 2013) or greater than (Richardson et al., 2000) that of the spring bloom. This production has been associated with significant atmospheric carbon dioxide drawdown (Kitidis et al., 2012), a high potential for carbon export to depth (Goldman, 1993; Kemp and Villareal, 2013; Sharples et al., 2001) and vital provision of sustenance for the pelagic food web (Benoit-Bird and McManus, 2012; Heath and Beare, 2008; Richardson et al., 2000; Scott et al., 2010). Thus, there is ample evidence attesting to the biogeochemical and ecological significance of the shelf sea SCM, highlighting a particular need for an improved understanding of the ecology of key SCM phytoplankton taxa.

This study focuses on the Western English Channel, a shallow (45–120 m) region of the NW European shelf with relatively weak tides that becomes stratified in the summer months (Dauvin, 2012; Pingree, 1980) and develops an SCM associated with the seasonal thermocline (Fishwick, 2017; Holligan and Harbour, 1977; Holligan et al., 1984b; Pingree, 1975). Hydrography in the Channel is heavily influenced by ambient weather conditions and by the tide (Pingree, 1980), and marked variation in environmental conditions can occur between years (Barnes et al., 2015; Pingree, 1980; Smyth et al., 2010; Southward et al., 2005b). Furthermore, the Western English Channel is reported to be one of the fastest warming regions of the NW European shelf (MCCIP et al., 2008). The Western Channel is a transition area between the boreal Baltic and North Sea continental systems, and the temperate Atlantic Oceanic system (Dauvin, 2012; Southward et al., 2005a), therefore changes in phytoplankton characteristic of this area brought about by environmental variation may be representative of the wider NW European shelf and possibly the temperate Atlantic.

Long term studies of interannual variability of phytoplankton communities in the Western Channel have primarily targeted surface waters. Several studies of long-term variability have used weekly samples taken at Station L4 at water depths of 10 m including those of Barnes et al. (2015); Barton et al. (2020); Tarran and Bruun (2015); Widdicombe et al. (2010). A 14 year record from L4 has been used to predict increasing frequency of dinoflagellate blooms with increased warming and stratification (Xie et al., 2015). Others have used data from the Continuous Plankton Recorder (CPR) which samples from 7m depth (Beaugrand et al., 2000; Beaugrand and Reid, 2003). However, there have been no studies of interannual variability of the SCM, whilst recent studies have shown the phytoplankton taxa of the SCM in the Western Channel to be distinct from the surface community (Barnett et al., 2019, 2022).

The present study investigated chlorophyll water column structure, phytoplankton community structure, and associated environmental conditions of the SCM sampled at a coastal repeat station in the Western English Channel, over 2–3 week periods, during the summers of 2013–2016, with the aim of establishing the environmental controls of interannual variability in SCM chlorophyll and phytoplankton community structure. The June – early July sampling interval coincides with the period during the development of summer stratification when the maximum strength of thermocline development coincides with maximal SCM chlorophyll as, for example, monitored by the weekly CTD casts at the Western Channel Observatory E1 buoy.

SCM chlorophyll structure is described in terms of peak chlorophyll concentration, vertical thickness (measured at half the peak chlorophyll concentration), and the 50 m to SCM peak chlorophyll ratio (concentration of chlorophyll within top 50 m divided by SCM peak chlorophyll; hereafter denoted by Chl_{50m}:Chl_{SCM} – a measure of the extent of chlorophyll dispersal through the water column). The SCM phytoplankton community structure was analysed by flow cytometry and by inverted light microscopy. Interannual variation in SCM chlorophyll structure and phytoplankton community composition is assessed, and the influence of environmental parameters, including (but not limited to) temperature, buoyancy frequency, the Richardson number, nutrient concentrations and ratios, salinity, wind speed and current velocity, is evaluated.

The repeat station sampling formed part of a more extensive field programme in the Western English Channel and the results from these surveys in 2013 and 2015 are published in Barnett et al. (2019, 2022) respectively, while those of 2014 and 2016 are presented in the supplementary material (see Table 1 for a summary of the full data sets collected over the 4 years, including data availability). These complementary studies include phytoplankton data from surface waters and deep waters (above and below the SCM) and the results are integrated in the discussion section. To provide a wider context, we also examined surface spring bloom (May–June) phytoplankton data from the Western Channel Observatory L4 buoy, (Widdicombe and Harbour, 2021) to assess any continuity or commonality with the spring bloom and SCM taxa.

2. Methods

2.1. Sampling

Samples were collected from the repeat site (50°05.670 N, 004°52.020 W ± 1.5 km; Fig. 1.) almost on a daily basis and over a range of different states of the semi-diurnal tide (Fig. 2.) in the summer stratified waters of the Western English Channel between 24th June – 4th July in 2013, 17th June – 3rd July in 2014, 22nd June – 2nd July in

Table 1
Summary of the full data sets collected over the 4 years of study including availability.

Year	Sampling dates	CTD cast and Chl *a* profiles	Phytoplankton samples analysed			Full data available
			SCM	Surface	Deep	
2013	24/6–4/7	52	12	4	4	Barnett et al. (2019) and supporting info.
2014	14/6–3/7	53	25	14	14	This paper and supplementary material
2015	19/6–2/7	40	40	11	10	Barnett et al. (2022) and supplementary material
2016	17/6–30/6	53	27	8	8	This paper and supplementary material

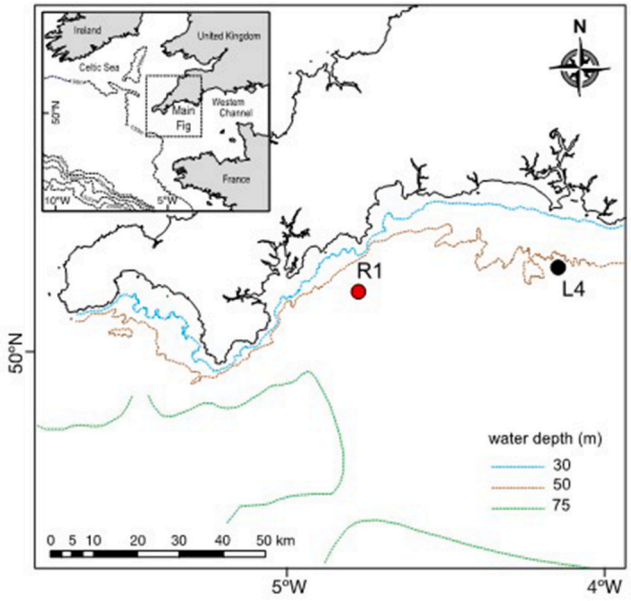

Fig. 1. Location of the repeat study site (R1) in the Western English Channel and also the Western Channel Observatory station L4.

2015 and 20th – 30th June in 2016. The repeat site had a water depth of approximately 66 m and was chosen based on past data revealing its location to be far enough away from the tidal mixing front to be permanently stratified in June/July, but also within a reasonable travel distance to permit regular sampling.

A SeaBird SBE19plus V2 conductivity, temperature, depth (CTD) probe mounted with a Wet Labs ECO FLNTU fluorometer (sensitivity: 0.025 μg chl/l; fluorescence excitation/emission wavelengths: 470/695 nm) was used to collect vertical water column profiles of temperature, salinity and chlorophyll-fluorescence. The CTD system was typically deployed at a descent/ascent rate of 0.01–0.1 m s^{-1} (rate slowed on approach to SCM), with a data acquisition rate of 2 Hz, which provided vertical resolution of 0.5–5 cm. Water samples were typically collected from the SCM during the up cast of the CTD frame using a Niskin sampling carousel (6 x 5 L Niskin bottles). Water samples were analysed for chlorophyll concentration, nutrient (nitrate, phosphate and silicate) concentrations, and phytoplankton community structure by CytoSense flow cytometry and inverted light microscopy. Note that samples for nutrient analysis and flow cytometric analysis were not collected in 2013.

Vertical profiles of buoyancy frequency, a measure of stratification, were computed from CTD data using SBE data processing software, where the buoyancy frequency was calculated using the Fofonoff adiabatic levelling method (Bray and Fofonoff, 1981). Current velocity and velocity shear was measured with a hull mounted RDI Workhorse 600 kHz ADCP, which combined with CTD density measurements allowed for calculation of the Richardson number, a measure of the static stability of the density stratification (Miles, 1961). Specifically, the Richardson number (Ri) was calculated for the depth interval of each SCM at the time of sampling, where Ri is defined as:

$$Ri = \frac{-g}{\rho}\frac{\delta\rho\delta z}{\delta U^2} = \frac{N^2}{S^2} \quad (6.1)$$

where N is buoyancy frequency (s^{-1}), S is velocity shear (s^{-1}), g is gravitational acceleration (9.81 m s^{-2}), ρ is *in situ* density (Kg m^{-3}), z is depth (m) and U is horizontal velocity (m s^{-1}).

Wind speed measurements were taken from the WCO L4 autonomous buoy situated at 50° 15.000 N, 004° 13.000 W (PML, 2017) for 2013 and 2014, but in 2015 and 2016 wind speed was logged by an onboard AIRMAR PB150 weather station. Daily rainfall measurements were collected by the PML meteorological station Omni Instruments 6″ tipping bucket rain gauge (RG200) (Smyth, 2017), and daily solar insolation measurements for the longitude and latitude of the repeat site were taken from NASA's CERES FLASHFlux project (NASA, 2018).

2.2. Determination of chlorophyll concentration

Samples for chlorophyll analysis were collected by passing 50 ml of water sample through a 25 mm Whatman GF/F filter and storing at −20 °C prior to analysis. Analysis was conducted as soon as possible after collection to avoid error associated with degradation of pigment at −20 °C (Graff and Rynearson, 2011). Chlorophyll was extracted in 90 % acetone via sonication and its concentration determined using a Turner Designs 10AU fluorometer based on the method of Welschmeyer (1994). The extracted sample was excited with blue light (436 nm) and the subsequent red fluorescence emission (680 nm) was recorded. Chlorophyll values were used for CTD fluorometer calibration, and permitted identification of where water samples were collected within the SCM (Fig. 3a and b and 4a and b).

2.3. Determination of nutrient concentrations

Samples for nitrate, phosphate and silicate analysis were collected by filtering water samples through a 25 mm Whatman GF/F filter into a 15 ml polypropylene tube, which was stored at −20 °C prior to analysis. Samples were slowly thawed in a fridge, with regular mixing to allow for depolymerisation of dissolved silicate. Nitrate, phosphate and silicate concentrations were determined following standard colourimetric techniques as described by Grasshoff (1976) and Kirkwood (1996), using a SEAL Analytical QuAAtro segmented flow AutoAnalyser. Detection limits for total nitrate, phosphate and silicate were 0.03 μmol l^{-1} (NIOZ, 2016), 0.01 μmol l^{-1} (NIOZ, 2015a) and 0.02 μmol l^{-1} (NIOZ, 2015b) respectively (Stinchcombe, 2017).

2.4. Phytoplankton community structure

Phytoplankton community structure within the SCM was assessed using inverted light microscopy and CytoSense flow cytometry. Flow cytometry allowed for quantification and description (based on fluorescence signatures) of the pico-phytoplankton and the entire nano-phytoplankton population, not achievable with light microscopy. Microscopy allowed for taxonomic identification of cells ≥10 μm, not possible with flow cytometry. Therefore, cells across the entire phytoplankton size range were represented in this study.

2.4.1. Phytoplankton identification, enumeration and biomass determination

Samples for phytoplankton analysis by microscopy were collected by decanting 50 ml of water sample into a darkened glass bottle and preserving in Lugol's iodine (1 % final concentration). Samples were analysed based on the methods of Utermöhl (1958), with 10 ml of preserved sample settled in a sedimentation chamber for 24 h and cells then identified and counted using a Brunel SP951 inverted trinocular light microscope (individual cells were counted in all cases, whether they be part of a colony/chain or solitary). Cells were counted irrespective of trophic status since although the term phytoplankton may strictly refer to obligate photoautotrophs, some dinoflagellate and ciliate taxa may be mixotrophic or heterotrophic and are routinely included in phytoplankton community counts (Olenina et al., 2006; Widdicombe et al., 2010).

Numerically dominant taxa (>50 cells per ml) were counted along a single middle transect under 100x or 250× magnification depending on cell size. Cryptophytes (>8 μm) and unidentified small naked dinoflagellates (10–20 μm and 20–25 μm) were also counted along a single middle transect at 250× magnification. All other cells ≥10 μm (cells generally unidentifiable below this threshold) were counted at 100×

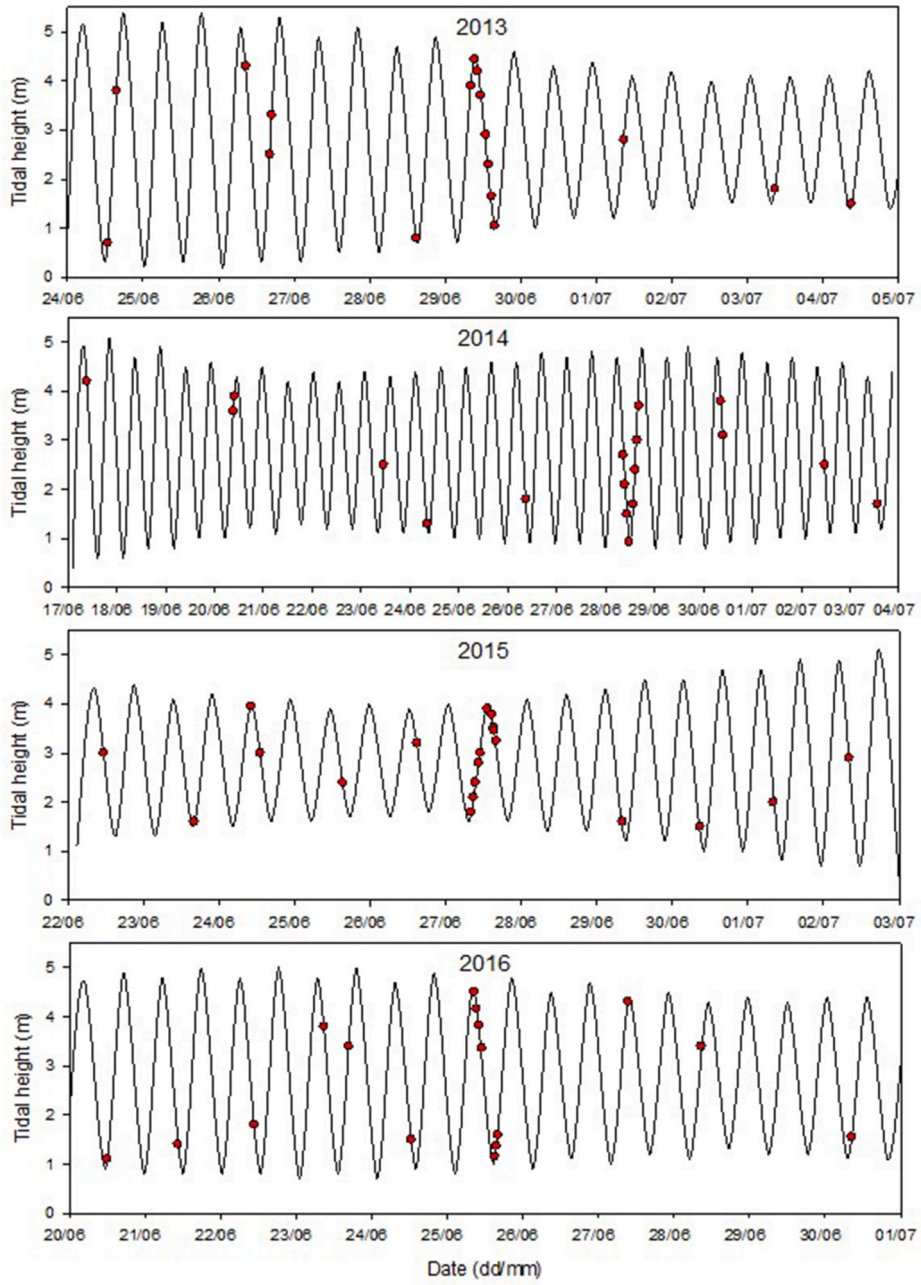

Fig. 2. Time series plots of tidal height in the Western English Channel during the summer survey periods of 2013, 2014, 2015 and 2016. Red circles indicate when vertical water column profiles were collected at the repeat study site. Labels on the x axis are positioned to correspond with midnight (UTC) on the date detailed. Tidal data was taken from tide tables for Falmouth (Tidetimes.co.uk, no date).

magnification during examination of the entire chamber base plate.

Cells were identified to a species level where possible, but were identified to the genus level when species could not be differentiated accurately, e.g. *Chaetoceros* spp., *Pseudo-nitzschia spp.*, *Rhizosolenia* spp. and *Thalassiosira* spp.. Any remaining unidentified diatoms were grouped as pennate or centric according to size (small: 20–40 μm length, medium: 40–65 μm length, large: 65–110 μm length; and small: 20–30 μm diameter, medium: 30–50 μm diameter, large: 60–150 μm diameter respectively). Unidentified dinoflagellates and ciliates were also grouped according to size and with reference to cell wall structure where appropriate (e.g. 10–20 μm and 20–25 μm naked dinoflagellates, 10–30 μm armoured dinoflagellates, and small (<20 μm), medium (20–40 μm) and large (>40 μm) aloricate ciliates). Some genera were classified into size categories, including *Pleurosigma* (small, medium and large: ~50 μm, 80–170 μm and 170–200 μm length), *Thalassiosira* (extra small, small, medium and large: <10 μm, 10–25 μm, 25–45 μm and >45 μm height), *Protoperidinium* (small, medium and large: 10–30 μm, 30–65 μm and 65–120 μm diameter) and *Rhizosolenia* (small, medium and large: ≤10 μm, 10–20 μm and >20 μm diameter). In the case of *Rhizosolenia*, small diameter cells appeared to be mainly *Rhizosolenia setigera* and *Rhizosolenia imbricata*, and medium and large diameter cells appeared to be mostly *Rhizosolenia imbricata* and *Rhizosolenia styliformis* across the four years.

Cell biovolume was derived for each taxon or taxon size category based on the geometric shapes and formulae of Olenina et al. (2006). Dimensions of at least 30 cells per taxon or taxon size category (only less for rare taxa) were measured with the open-source software 'ImageJ'. Cell carbon concentrations were estimated using the carbon - biovolume relationships of Menden-Deuer and Lessard (2000).

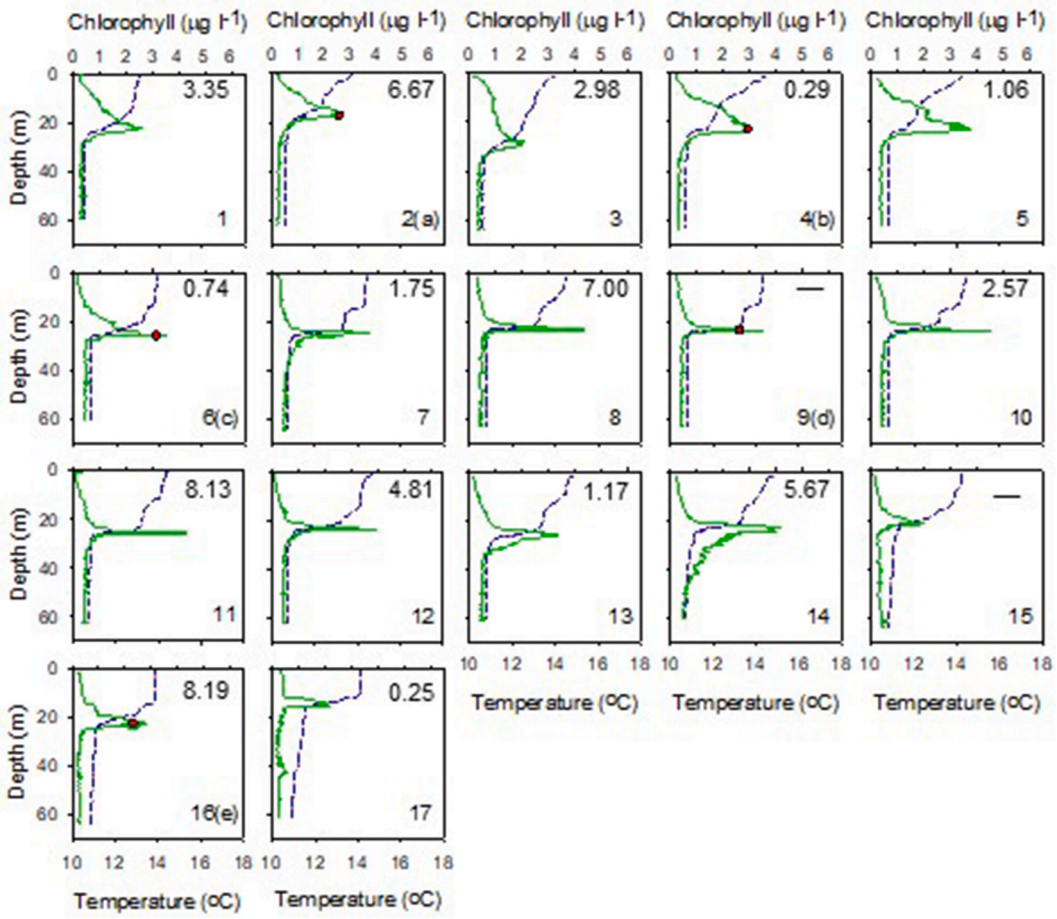

Fig. 3. Temperature and chlorophyll profiles at the repeat site in the Western English Channel (cast numbers given in the bottom right hand corner of each plot, with phytoplankton sample IDs in brackets) collected during (a) June/July 2013 and (b) June/July 2014 (further details provided in Supplementary Table 2). The green line represents chlorophyll concentration determined from CTD chlorophyll-fluorescence, the blue dashed line temperature and the red circles where water samples were collected for phytoplankton analysis. The Richardson number for the thermocline level is at the top of each plot.

2.4.2. *Flow cytometric analysis of the phytoplankton community*

Samples for phytoplankton analysis by flow cytometry were collected by decanting 10 ml of water sample into a polypropylene tube, immediately fixing with glutaraldehyde (0.25 % final concentration) and freezing at −80 °C. Samples were analysed with a CytoBuoy CytoSense flow cytometer and CytoUSB v5.7.5.7 data acquisition software, using two sets of data acquisition settings; one optimal for small phytoplankton (pico-phytoplankton: <2 µm) and the other for larger phytoplankton (meso- and micro phytoplankton: 20–2000 µm; and nano-phytoplankton: 2–20 µm). Pico-phytoplankton data was acquired using a sideways scatter (SWS) trigger (25 mV) at a flow rate of 0.1 µl s^{-1} for 10000 cells, and pico-particles with a red fluorescence (RFL) signal <10 mV were manually removed from the dataset to ensure exclusion of non-phytoplankton pico-particles/debris/electronic noise. Meso-, micro- and nano-phytoplankton data was acquired using a red fluorescence trigger (30 mV) at a flow rate of 10 µl s^{-1} for 150 s or 10000 cells. Cell size derived from forwards scatter (FWS) was calibrated using Thermo Fisher Scientific nonfluorescent polystyrene microspheres of a range of diameters (1, 2, 6, 10, 15 µm).

During data acquisition the CytoSense instrument recorded particle pulse shapes of FWS, SWS, RFL and orange fluorescence (OFL), enabling description of the phytoplankton community based on scatter and fluorescence properties using CytoClus v4.3.1.1 data processing software. For each sample a cytogram of total OFL vs. total RFL (TRFL) was constructed to identify cells containing phycoerythrin secondary photopigments (Jeffrey and Vesk, 1997), and a cytogram of total FWS and TRFL was generated to identify cell size. Clusters of orange fluorescing pico-phytoplankton (hereafter orange pico-phytoplankton), red fluorescing pico-phytoplankton (hereafter red pico-phytoplankton), orange fluorescing nano-phytoplankton (hereafter orange nano-phytoplankton), red fluorescing nano-phytoplankton (hereafter red nano-phytoplankton), and micro- and meso-phytoplankton could thus be resolved. As TRFL was calculated for each cell, the TRFL of the entire phytoplankton population and of each phytoplankton cluster could be determined and was used as a proxy for chlorophyll concentration, which in turn is a proxy for biomass. Note that as samples for flow cytometric analysis were not collected in 2013, most nano-phytoplankton <10 µm and all pico-phytoplankton within the SCM community during 2013 are not represented in this study.

2.5. *Statistical analysis*

One way analysis of variance (ANOVA) with post hoc Dunn's pairwise multiple comparison analysis was performed using SigmaPlot 13.0 software to identify significant interannual differences in the SCM chlorophyll structure characteristics of thickness (measured at half peak intensity of the chlorophyll signal), peak chlorophyll concentration and Chl_{50m}:Chl_{SCM}. One way ANOVA with post hoc Dunn's pairwise multiple comparison analysis was also performed to detect significant interannual changes in environmental variables that had the potential to significantly influence chlorophyll structure. These variables included SCM depth (as a proxy for mixed layer depth), SCM temperature

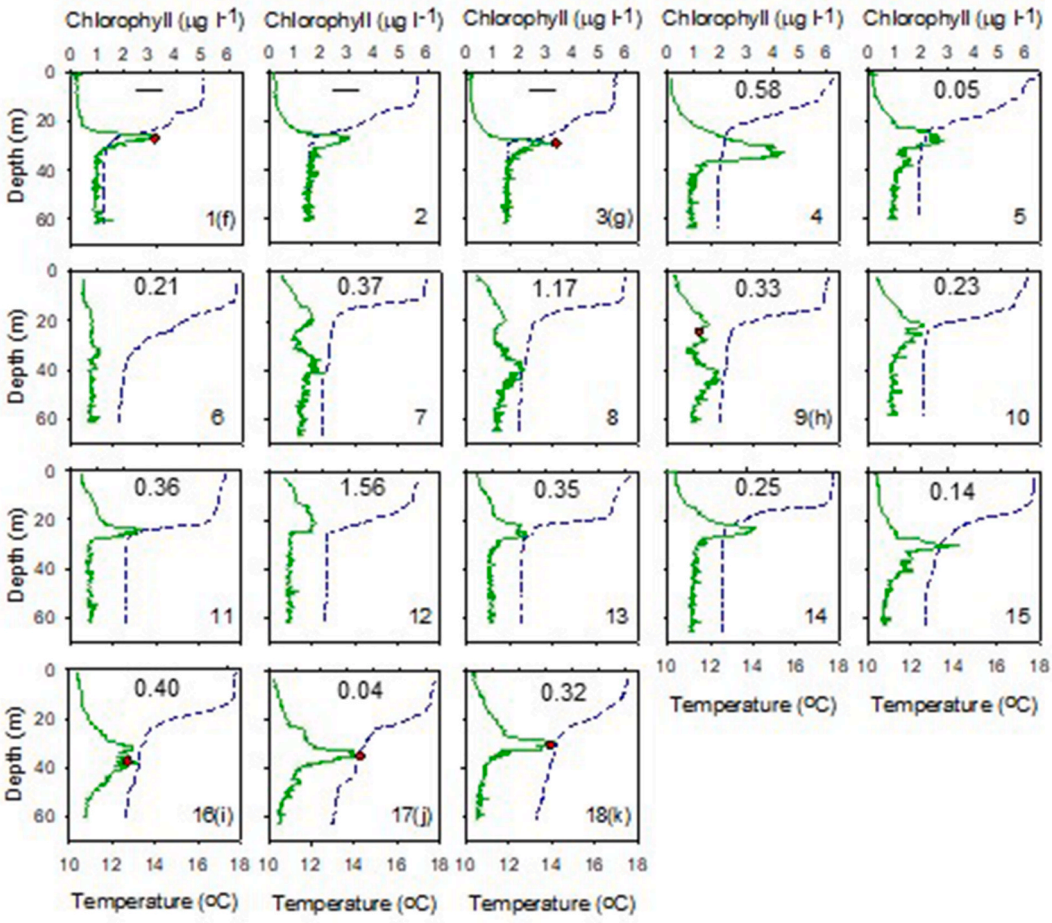

Fig. 3. (*continued*).

(measured at maximal chlorophyll concentration), buoyancy frequency (maximum value associated with the thermocline), Richardson number (determined for the depth interval of the SCM), wind speed (30–90 min before profile), current velocity (water column averaged), solar insolation (day before profile) and SCM nitrate concentration (nutrient status indicator).

Phytoplankton community structure was investigated using PRIMER v6 software (Clarke and Gorley, 2006; Clarke and Warwick, 2001). Statistical analysis was conducted on phytoplankton carbon biomass data derived from microscope analysis of Lugol's preserved phytoplankton samples, and on phytoplankton TRFL (as a proxy for biomass) data collected from CytoSense cytometric analysis. Biomass/biomass proxy data was used instead of abundance data because it provides a more accurate representation of community structure when the community includes taxa of a range of different sizes, and because biomass is of more biogeochemical relevance than abundance (Paasche, 1960). Data was standardised by dividing carbon biomass/TRFL values by the total biomass/TRFL for a given sample, then normalised by square root transformation to moderate the influence of dominant phytoplankton on similarity between samples. To explore similarity of community structure among SCM samples collected at the repeat site over the years of study, cluster analysis with SIMPROF (Similarity Profile Analysis; significance level at 0.05) was performed, using the Bray-Curtis index as the measure of similarity. A threshold of 61 % similarity was applied to group microscope analysed phytoplankton samples by year, and a threshold of 87 % similarity was used to group CytoSense analysed phytoplankton samples by year. Post hoc analysis of similarity (one-way ANOSIM) was applied to determine the level of separation of community structure between years (given by global R value, where values close to 0 indicate no separation and values close to 1 indicate high separation), and a non-metric multi-dimensional scaling (nMDS) plot was used to visually display the separation between samples. Samples with greater community resemblances were spatially closer than ones that were less similar. The stress level of the nMDS is a measure of how accurate a representation the ordination is, where a value below 0.2 is considered to indicate a good fit (Zuur et al., 2007). SIMPER (Similarity Percentage Analysis) was performed to investigate similarities within year clusters. SIMPER output was also used to identify contributions of each taxon/phytoplankton cell size and fluorescence (red/orange) group to the (average) overall similarity within and dissimilarity between clusters, with a limit of 90 % cumulative contribution.

To analyse the effects of environmental variables on community structure assessed by microscopy (carbon biomass data), and community structure assessed by flow cytometry (TRFL data), Redundancy Analysis (RDA; a constrained form of the linear ordination technique of principle component analysis) was performed using CANOCO 4.5 software (Lepš and Šmilauer, 2003). This multivariate analysis method selects the linear combination of environmental variables that produces the lowest total residual sum of squares in the phytoplankton data (Peterson et al., 2007). RDA was chosen because a Detrending Canonical Correspondence Analysis (DCCA) had identified the largest gradient in the environmental variables to be less than 2 standard deviation units, indicating a unimodal ordination method (Canonical Correspondence Analysis; CCA) would not be appropriate (Lepš and Šmilauer, 2003). For the RDA using carbon biomass phytoplankton data, log transformation was performed, and only taxa that contributed more than 5 % of community biomass were selected for the analysis. For the RDA using TRFL data, values were standardised to the total community TRFL for each

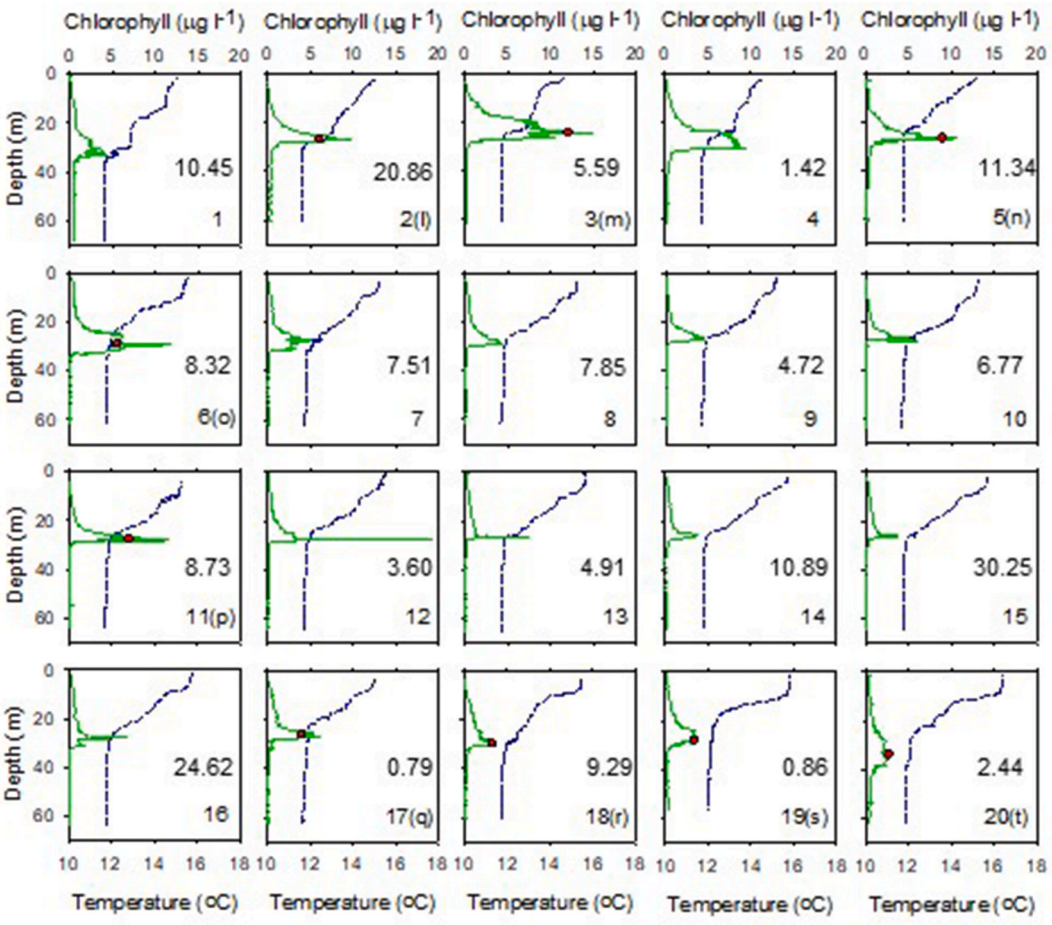

Fig. 4. Temperature and chlorophyll profiles at the repeat site in the Western English Channel (cast numbers given in the bottom right hand corner of each plot, with phytoplankton sample IDs in brackets) collected during (a) June/July 2015 and (b) June 2016 (further details provided in Supplementary Table 2). The green line represents chlorophyll concentration determined from CTD chlorophyll-fluorescence, the blue dashed line temperature and the red circles where water samples were collected for phytoplankton analysis. The Richardson number for the thermocline level is at the middle-right of each plot.

given sample, then square root transformed (ter Braak and Šmilauer, 2002). Forward-selection was used to determine environmental variables that significantly influenced phytoplankton distribution and community structure when analysed singly (marginal effects) or together with other forward-selected variables (conditional effects), and Monte Carlo permutation tests provided a measure of statistical significance of each of the forward-selected environmental variables applied in the RDA.

3. Results

The results of the various measurements are presented in Figs. 3–12 and Tables 1–4 and in the Supplementary material. In this section the results of the statistical analyses are presented.

3.1. Environmental influence on SCM chlorophyll structure

SCM peak chlorophyll concentration was significantly higher in 2015 (average of 7.3 µg l^{-1}) compared to 2013 ($p = 0.010$), 2014 ($p < 0.001$) and 2016 ($p < 0.001$), when average peak chlorophyll values were 3.3, 2.7 and 3.1 µg l^{-1} respectively (Fig. 5b and Table 2). Chlorophyll concentration within the top 50 m of the water column relative to SCM peak chlorophyll concentration (Chl_{50m}:Chl_{SCM}) was significantly less in 2013 and 2015 (average ratios of 10.5 and 7.0) compared to 2014 ($p = 0.003$ and <0.001 respectively) and 2016 ($p = 0.015$ and <0.001 respectively), when Chl_{50m}:Chl_{SCM} averaged 21.7 and 19.3 respectively (Fig. 5c). Thus, chlorophyll was generally more dispersed in the water column in 2014 and 2016 compared to 2013 and 2015.

The higher peak SCM chlorophyll concentrations and larger contributions of the SCM to water column chlorophyll in 2015 coincided with significantly greater stability at the depth interval of the SCM (average Ri of 9.07) than in 2014 ($p < 0.001$) and 2016 ($p < 0.001$) (Fig. 6a and Table 2), despite significantly lower stratification strength in 2015 ($p < 0.001$; Table 2). The increased stability in 2015 coincided with lower current velocities (average current velocity of 0.14 m s^{-1}) than in other years (2013: $p = 0.011$, 2014: $p = 0.014$, and 2016: $p < 0.001$) when current velocity was around 0.10 m s^{-1} faster on average (Fig. 6c and Table 2). Thus, the lower peak SCM chlorophyll concentrations with higher Chl_{50m}:Chl_{SCM} in 2014 and 2016 compared to 2015 may be attributed to significantly reduced stability, with Richardson numbers averaging 0.42 and 0.62 respectively (Fig. 6a and Table 2). In 2013 the significantly lower Chl_{50m}:Chl_{SCM} relative to 2014 and 2016 may be ascribed to greater stability (average Ri of 3.64) than in 2014 ($p = 0.004$) and 2016 ($p = 0.048$) (Fig. 6a and Table 2). Despite greater stability in 2013, SCM peak chlorophyll concentrations were comparatively low, coinciding with significantly lower SCM temperatures than in any other year ($p < 0.02$) (Fig. 6d and Table 2). The data from 2013 do, however, show that the thinnest and most intense SCM (SCMTLs) all occur when the wind speed was less than 8 ms^{-1} suggesting that lower wind speeds favoured their development (Barnett et al., 2019).

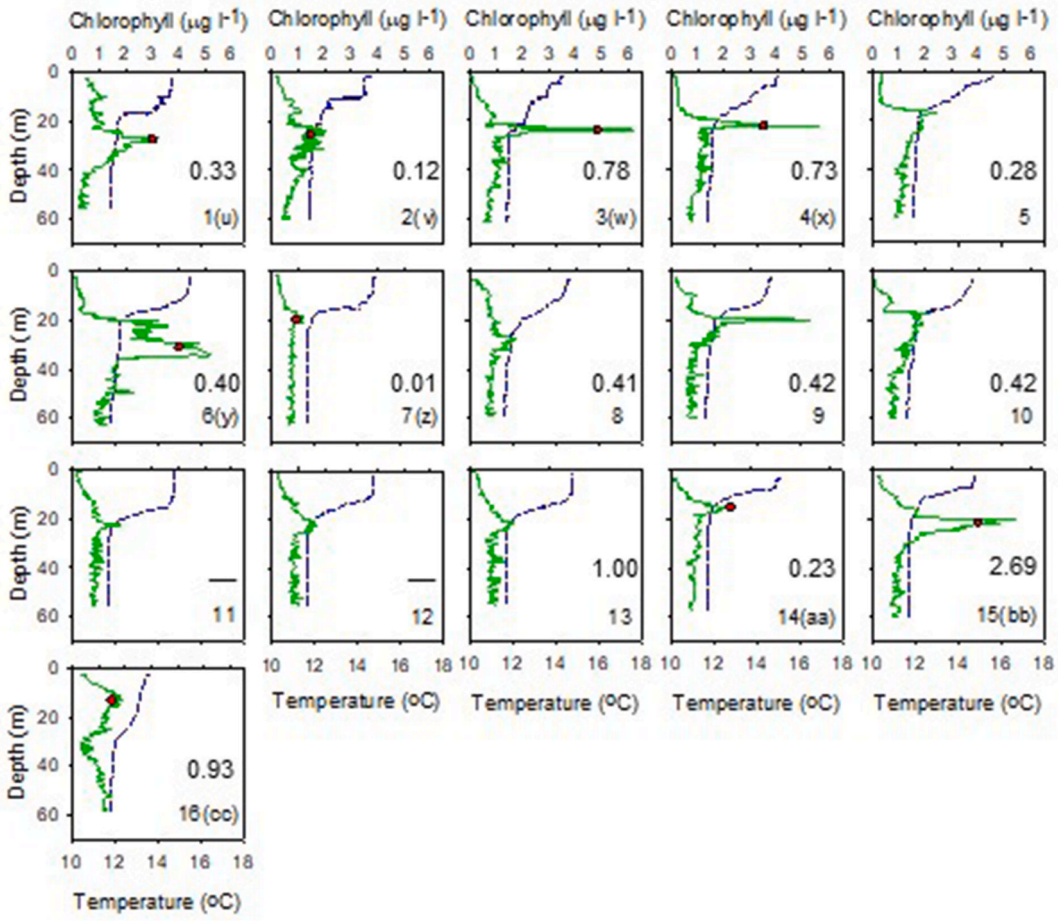

Fig. 4. (*continued*).

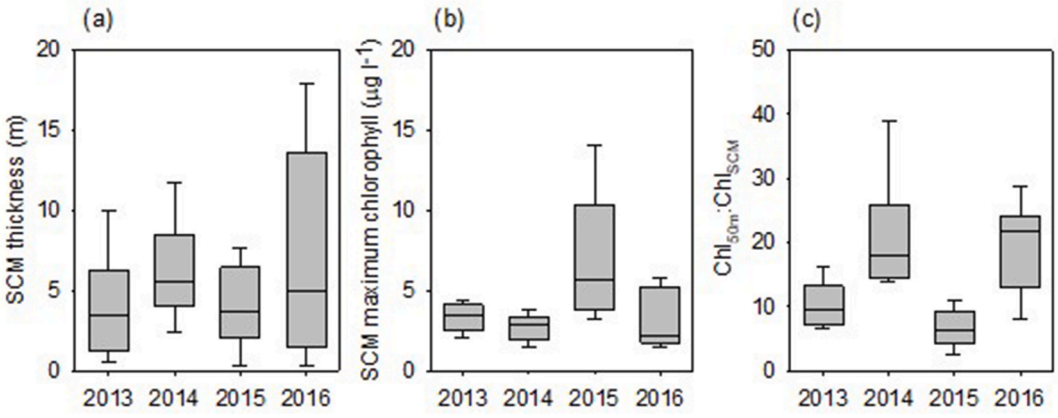

Fig. 5. Boxplots (median, upper and lower quartile, and minimum and maximum values) of the SCM characteristics of (a) thickness, (b) peak chlorophyll and (c) Chl50m:ChlSCM for 2013–2016.

Other environmental parameters (Table 2) that significantly changed during the 4 years of study and had potential to influence SCM chlorophyll structure include nutrient concentration ($p = 0.017$), solar insolation ($p = 0.012$), SCM depth ($p < 0.001$) and wind speed ($p = 0.049$). However, a robust association between these parameters and changing SCM chlorophyll structure over the years of study was not found.

3.2. SCM phytoplankton community structure: cluster analysis

3.2.1. Community structure by flow cytometry

The relative contributions of the five cell size and fluorescence phytoplankton groups derived by flow cytometry (micro-and meso-phytoplankton, red nano-phytoplankton, orange nano-phytoplankton, orange pico-phytoplankton and red pico-phytoplankton) differed between years (Fig. 7). A cluster analysis with ANOSIM using CytoSense TRFL data identified the SCM phytoplankton community to be statistically distinct between the years of 2014–2016 ($p = 0.001$), and a global

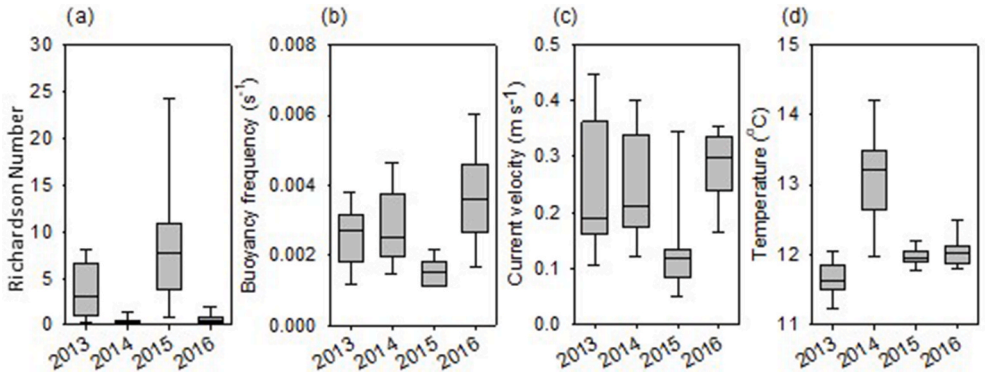

Fig. 6. Boxplots (median, upper and lower quartile, and minimum and maximum values) for 2013 - 16 of environmental factors (a) Richardson number, (b) buoyancy frequency, (c) current velocity and (d) SCM temperature.

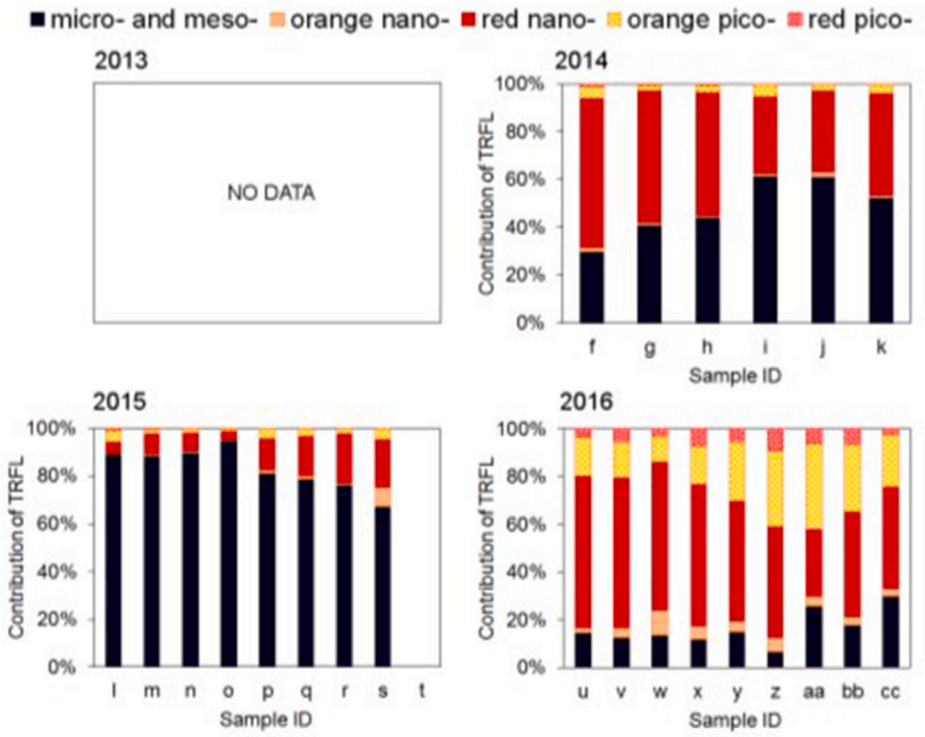

Fig. 7. Phytoplankton community structure within the SCM at the repeat site in the Western English Channel in summer (June/July) 2014, 2015 and 2016 (details in Table 3), based on data compiled using CytoSense flow cytometry (no phytoplankton samples for CytoSense flow cytometry analysis were collected in 2013 or for sample t in 2015).

R of 0.93 (R statistic from pairwise tests varied from 0.81 to 1) indicated the sample clusters for each year were well separated. nMDS analysis provided a 2D spatial representation of the separation between samples from 2014, 2015 and 2016 based on their phytoplankton TRFL values, and a stress level of 0.03 verified the representation to be accurate (Fig. 8).

In 2014 average similarity of samples was 90.9 %, and the top three contributors of this similarity were micro- and meso-phytoplankton (40.5 %), red nano-phytoplankton (39.7 %) and orange pico-phytoplankton (10.8 %). In 2015 average similarity of samples was 89.8 %, and the top three phytoplankton groups responsible for similarity were micro- and meso-phytoplankton (62.5 %), red nano-phytoplankton (19.0 %) and orange pico-phytoplankton (9.6 %). In 2016 average similarity was 89.4 %, and the top three phytoplankton groups accountable for this similarity were red nano-phytoplankton (36.7 %), orange pico-phytoplankton (22.8 %) and micro- and meso-phytoplankton (19.2 %) (Fig. 7 and Table 3).

3.2.2. *Community structure by microscopy*

The ≥10 μm community within the SCM identified using light microscopy was either predominantly a mix of diatoms and dinoflagellates (2013, 2014 and 2016) or strongly dominated by dinoflagellates (2015) (Fig. 9).

A cluster analysis with ANOSIM using biomass data showed the SCM phytoplankton community to be statistically distinct in each year (p = 0.001), and a global R of 0.98 (R statistic from pairwise tests varied from 0.94 to 1) indicated the sample clusters for each year were well separated. An nMDS analysis provided a 2D spatial representation of the separation between samples from 2013, 2014, 2015 and 2016 based on their phytoplankton biomass values, and a stress level of 0.1 verified the representation to be accurate (Fig. 10). Taxa whose cumulative contribution to similarity within a year was approximately 90 % are given in

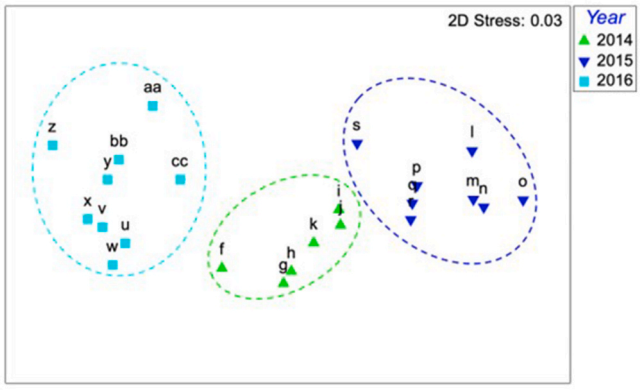

Fig. 8. nMDS plot representing the similarity in SCM phytoplankton community structure at the repeat site in the Western English Channel between 2014 (green triangles), 2015 (dark blue inverted triangles) and 2016 (light blue squares), based on CytoSense TRFL values. The 2D stress value is included, dotted outlines represent a sample similarity level of 87 % and each sample is labelled with its sample ID.

Supplementary Table 1.

In 2013, average similarity of samples was 70.4 %, and the top five taxa to account for similarity were small *Pseudo-nitzschia spp.* (20.0 %), 10–20 μm naked dinoflagellates (12.4 %), *Tripos lineatus* (10.5 %), *Chaetoceros* spp. (6.0 %) and *Diplopsalis lenticula* (5.6 %). In 2014 average similarity of samples was 66.9 %, and the top five contributors of this similarity were 20–25 μm naked dinoflagellates (9.3 %), 10–20 μm naked dinoflagellates (8.4 %), *Tripos lineatus* (8.0 %), *Gyrodinium* spp. (6.6 %) and *Leptocylindrus danicus* (6.5 %). In 2015, average similarity of samples was 67.6 %, and the top five taxa responsible for similarity were *Tripos fusus* (18.5 %), large aloricate ciliates (8.0 %), 10–20 μm naked dinoflagellates (5.2 %), *Tripos lineatus* (4.8 %) and *Proboscia truncata* (4.7 %). In 2016 average similarity was 69.6 %, and the top 5 contributors of this similarity were *Chaetoceros* spp. (10.5 %), 10–20 μm naked dinoflagellates (10.4 %), large aloricate ciliates (8.8 %), 20–25 μm naked dinoflagellates (8.8 %) and *Protoperidinium* spp. (5.9 %) (Fig. 9 and Table 4).

3.3. Environmental influence on SCM phytoplankton community structure from redundancy analysis

3.3.1. Environmental influence on community structure by flow cytometry

Environmental variables that accounted for the variance in TRFL of the phytoplankton groups derived by flow cytometry were assessed (Fig. 11 and Supplementary Table 3). In the ordination diagram (Fig. 11) the degree of association between the different phytoplankton groups and environmental variables is indicated by their proximity. Close proximity in the same or opposite direction indicates positive or negative correlation, respectively, and the longer the arrow the stronger the correlation, whereas no proximity suggests a weak or no relationship. All canonical axes explained 99.9 % of the variance ($p = 0.003$), suggesting that the measured environmental variables explained almost all of the variation in the structure of the SCM community as assessed by flow cytometry over the 3 years, when all axes were analysed together (Supplementary Table 3). The eigenvalues (λ, dimensionless; Supplementary Table 3) associated with the environmental variables are shown in the order of the variance in the data they explained individually (marginal effects – λ_1 in Supplementary Table 3), along with the significance of that variable (according to forward selection and a Monte Carlo permutations test; conditional effects - λ_a in Supplementary Table 3). The variables that were considered to be significant were buoyancy frequency (Buoyancy; $\lambda_a = 0.41$, $p = 0.001$), Richardson number (Ri; $\lambda_a = 0.19$, $p = 0.002$) and silicate concentration (Si; $\lambda_a = 0.15$, $p = 0.002$).

The SCM community was consistently dominated by micro- and meso-phytoplankton when waters were highly stable with relatively higher SCM silicate concentration (2015 - mean Ri of 9.07, and mean silicate of 1.14 μmol l^{-1}; Table 2). Red nano-phytoplankton accounted for greater proportions of the community in waters with low stability (2014 and 2016 – mean Ri of 0.42 and 0.62 respectively; Table 2). Orange nano- and all pico-phytoplankton contributed more to the community when silicate concentration in the SCM was lowest and when stratification was strongest (2016 - mean silicate of 0.61 μmol l^{-1} Table 2) (Fig. 11).

3.3.2. Environmental influence on community structure by microscopy

Environmental variables that accounted for the variance in the carbon biomass of selected taxa (biomass greater than 5 % of community) were investigated (Fig. 12 and Supplementary Table 4). All canonical axes explained 87.8 % of the variance ($p = 0.001$), indicating the measured environmental variables explained the majority of the variation in the structure of the SCM community as identified by microscopy over the 4 years samples were collected, when all axes were analysed together (Supplementary Table 4). The eigenvalues (λ, dimensionless; Supplementary Table 4) associated with the environmental variables are shown in the order of the variance in the data they explained individually (marginal effects – λ_1 in Supplementary Table 4), along with the significance of that variable (according to forward selection and a Monte Carlo permutations test; conditional effects - λ_a in Supplementary Table 4). The variables that were considered to be significant were silicate concentration (Si; $\lambda_a = 0.18$, $p = 0.001$) temperature (Temp; $\lambda_a = 0.12$, $p = 0.002$), Richardson number (Ri; $\lambda_a = 0.10$, $p = 0.002$), nitrate to phosphate ratio (Ni:P; $\lambda_a = 0.05$, $p = 0.01$), nitrate to silicate ratio (Ni:Si; $\lambda_a = 0.06$, $p = 0.007$) and phosphate concentration (P; $\lambda_a = 0.04$, $p = 0.038$).

Dinophysis acuminata and small naked dinoflagellate biomass was present in relatively similar amounts in all years but increases in biomass were found in association with lower stability (Fig. 12). Ciliates were a noteworthy inhabitant of the SCM in all years, but increased biomass was most strongly correlated with greater silicate concentrations (Fig. 12). In 2013 and 2016, smaller diatoms (generally <400 μm^3 in volume: *Chaetoceros* spp. and *Pseudo-nitzschia spp.*) and smaller dinoflagellates (<15000 μm^3 in volume: *Prorocentrum micans* and *Diplopsalis lentiula*) were common, found in SCM waters that were relatively cooler (mean temperature of 11.6 and 12.1 °C in 2013 and 2016 respectively; Table 2), and in the case of 2016, had the lowest silicate concentrations (mean of 0.61 μmol l^{-1}) and Ni:P ratios (mean of 1.77) (Fig. 12). Nutrient data is not available for 2013, thus no relationship between taxa and nutrient concentrations or ratios can be derived. In 2014, large *Rhizosolenia* spp., *Lauderia annulata*, *Leptocylindrus danicus*, *Gyrodinium* spp. and *Polykrikos* spp., particularly common within the SCM in this year, were strongly correlated with warmer waters and greater silicate concentrations and Ni:P ratios (mean temperature of 13.1 °C, ≥1 °C warmer on average than in other years, and mean silicate concentration and Ni:P ratio of 1.39 μmol l^{-1} and 6.48 respectively; Table 2) (Fig. 12). In 2015 the SCM community was typically dominated by *Tripos fusus*, strongly correlated with high stability and associated with relatively increased phosphate and silicate concentrations (mean Ri of 9.07, and mean phosphate and silicate of 0.15 and 1.14 μmol l^{-1} respectively; Table 2). Extra small *Thalassiosira* spp., *Dinophysis acuta* and *Dictyocha* spp., also common in 2015, were similarly related to these conditions (Fig. 12).

4. Discussion

4.1. Influence of environmental variation on SCM chlorophyll structure

Chlorophyll structure of the SCM, assessed in terms of thickness, peak chlorophyll concentration and Chl_{50m}:Chl_{SCM}, varied significantly over the four years of study, notably with higher peak SCM chlorophyll

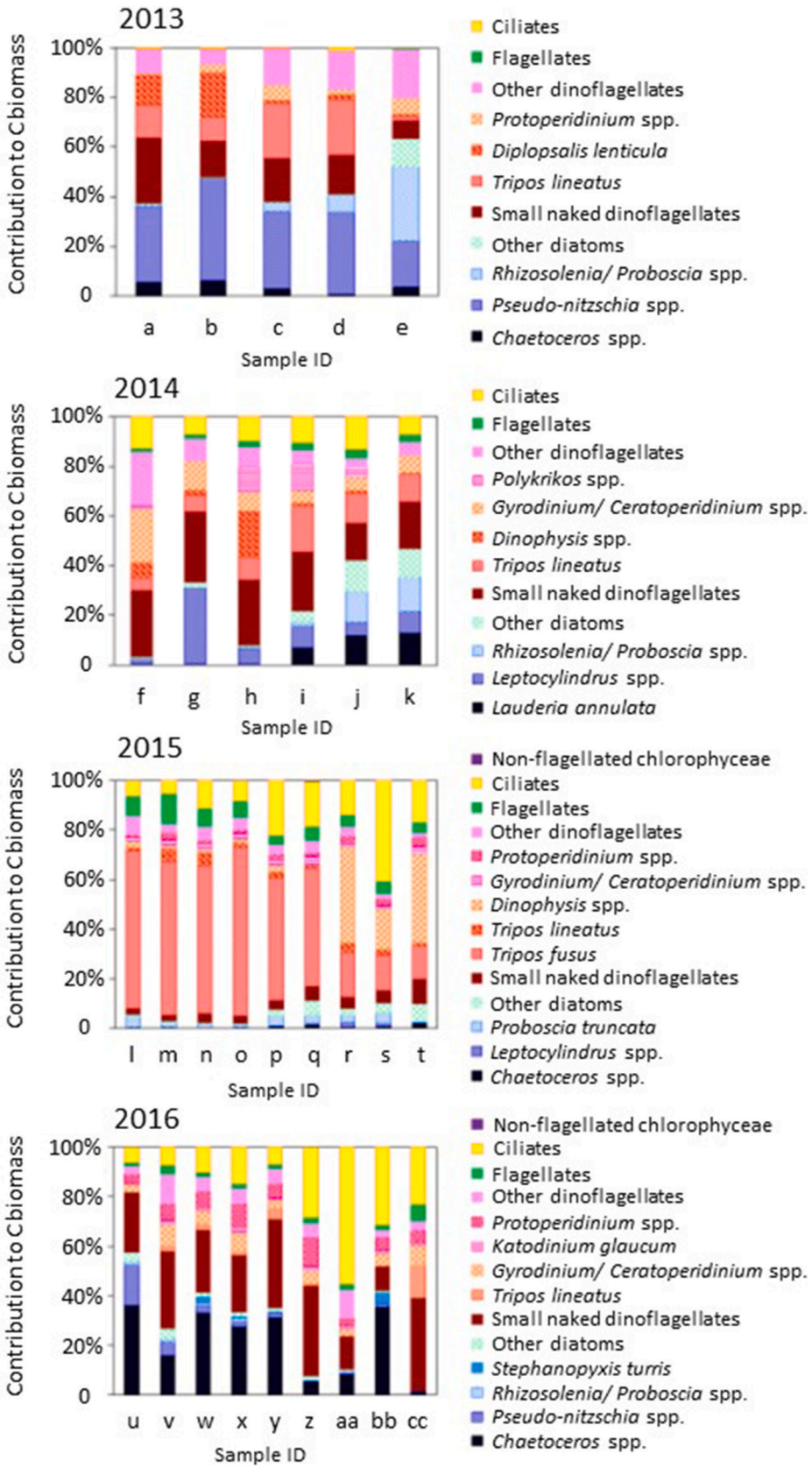

Fig. 9. Phytoplankton community structure within the SCM at the repeat site in the Western English Channel in summer (June/July) 2013, 2014, 2015 and 2016 (details in Table 4), based on data compiled using inverted light microscopy. Diatom taxa carbon biomass is indicated by blue colouration and dinoflagellate taxa carbon biomass by red colouration. Full phytoplankton counts are given in the supplementary material.

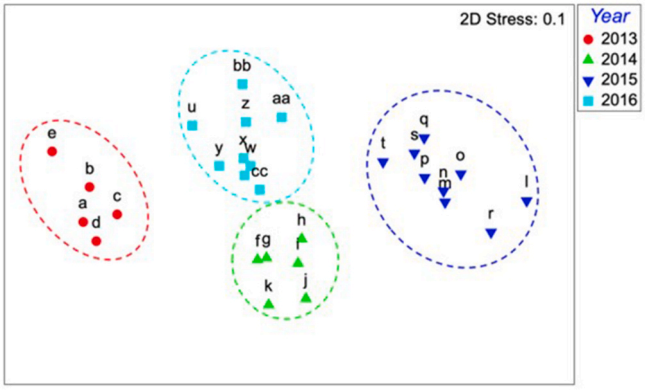

Fig. 10. nMDS plot representing similarity in SCM phytoplankton community structure at the repeat site in the Western English Channel between 2013 (red circles), 2014 (green triangles), 2015 (dark blue inverted triangles) and 2016 (light blue squares), based on carbon biomass data from inverted light microscopy. The 2D stress value is included, dotted outlines signify a similarity level of 61 % and each sample is labelled with its sample ID.

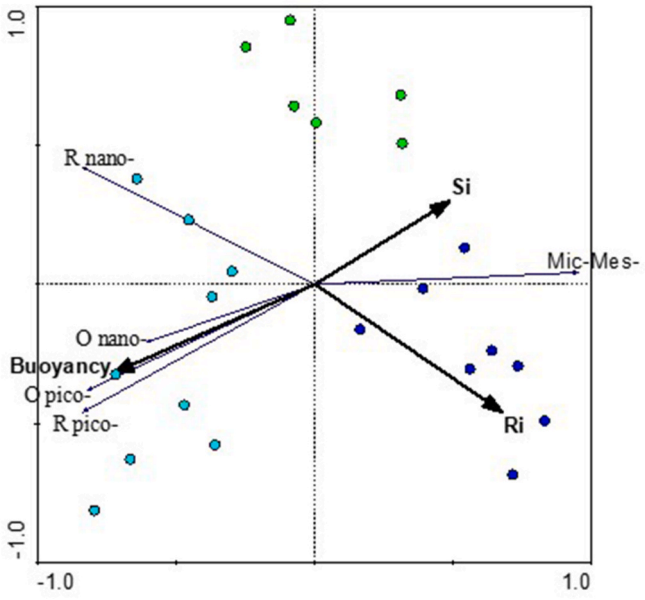

Fig. 11. Ordination diagram generated from redundancy analysis (RDA) of the flow cytometry results. The triplot shows cell size and fluorescence (red/orange) phytoplankton groups (thin blue lines), environmental variables identified to describe a significant portion of the variability in the phytoplankton data by the RDA (thick black lines), and samples (closed circles, where colours refer to year groups: green = 2014, dark blue = 2015, and light blue = 2016). Mic-Mes- refers to micro- and meso-phytoplankton, O nano-is orange nano-phytoplankton, R nano-is red nano-phytoplankton, O pico-is orange pico-phytoplankton, and R pico-is red pico-phytoplankton. The significant environmental variables included buoyancy frequency (buoyancy; s^{-1}), Richardson number (Ri) and silicate concentration (Si; μmol l^{-1}).

concentrations in 2015 (mean and standard deviation of 7.3 ± 4.4 μg l^{-1}; Table 2) relative to other years, and higher Chl_{50m}:Chl_{SCM} in 2014 (21.7 ± 9.1) and 2016 (19.3 ± 7.0) compared to 2013 (10.5 ± 3.5) and 2015 (7.0 ± 4.0) (Fig. 5 and Table 2; details provided in Supplementary Table 2).

4.1.1. *Influence of water column stability (Richardson number)*

In 2013 and 2015 stability at the depth interval of the SCM was significantly greater than in 2014 and 2016 (Fig. 6a), and this higher

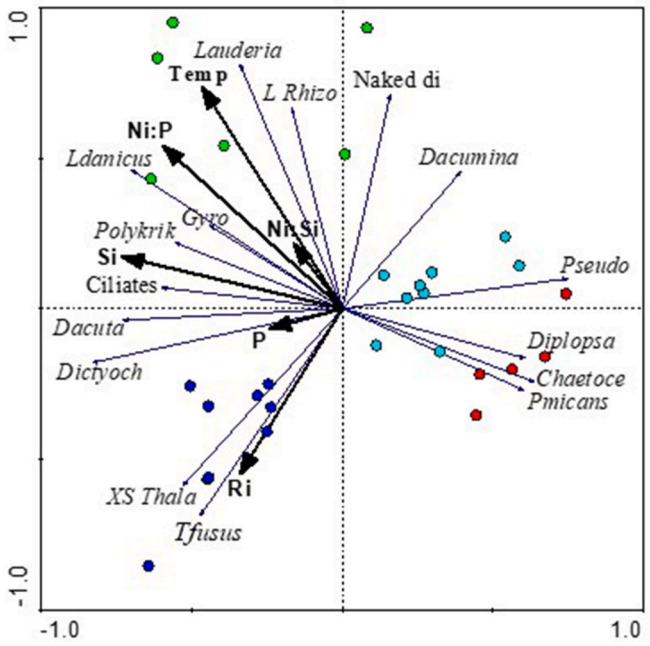

Fig. 12. Ordination diagram generated from redundancy analysis (RDA) from the results of microscopy. The triplot shows taxa carbon biomass (thin blue lines), environmental variables identified to describe a significant portion of the variability in the phytoplankton taxa data by the RDA (thick black lines), and samples (closed circles, where colours refer to year groups: red = 2013, green = 2014, dark blue = 2015, and light blue = 2016). Only species with ≥15 % goodness of fit with the environmental variables are included in the ordination diagram. Naked di refers to small (10–25 μm) naked dinoflagellates not identified to genus/species, *Dacumina* is *Dinophysis acuminata*, *Pseudo* is *Pseudo-nitzschia* spp., *Diplopsa* is *Diplopsalis lenticula*, *Chaetoce* is *Chaetoceros* spp., *Pmicans* is *Prorocentrum micans*, *Tfusus* is *Tripos fusus*, *XS Thala* is Thalassiosira spp. < 10 μm height, *Dictyoch* is *Dictyocha* spp., *Dacuta* is *Dinophysis acuta*, *Polykrik* is *Polykrikos* spp., *Gyro* is *Gyrodinium* spp., *Ldanicus* is *Leptocylindrus danicus, L Rhizo* is *Rhizosolenia* spp. > 20 μm in diameter, and *Lauderia* is *Lauderia annulata*. The significant environmental variables included silicate concentration (Si; μmol l^{-1}), temperature (temp; °C), Richardson number (Ri), nitrate to phosphate ratio (Ni:P), nitrate to silicate ratio (Ni:Si) and phosphate concentration (P; μmol l^{-1}). Note no nutrient data is available for 2013, thus no relationship between taxa and nutrient concentrations or ratios can be derived based on this ordination.

stability coincided with lower Chl_{50m}:Chl_{SCM} (less chlorophyll dispersal in the water column) (Fig. 5c), and in 2015 also coincided with particularly high peak chlorophyll concentrations (Fig. 5b). Several of the Ri values for 2014 and 2016 are less than 0.25, values taken as the necessary condition for the onset of turbulence (Miles, 1961; Sharples and Simpson, 2012). Stability was the only variable that had an association with chlorophyll structure in all four years, suggesting that in any given year, the degree of velocity shear at the depth interval of the SCM was key for governing chlorophyll structure. The strength of stratification, given by buoyancy frequency (Table 2), was also found to be significantly lower in 2015 (Fig. 6b) compared to the other years but there was no consistent relation of chlorophyll structure to buoyancy frequency over the 4 years.

The decreased stability and turbulent mixing in 2014 and 2016 are associated with lower Chl_{50m}:Chl_{SCM}, indicating more dispersal of chlorophyll through the water column. This is mainly manifest as increased chlorophyll beneath the SCM, suggesting erosion of, and sedimentation from the SCM. The greater stability in 2013 and 2015, likely minimised chlorophyll dispersal from the SCM to the surrounding water column and is consistent with the lower Chl_{50m}:Chl_{SCM} in 2013 and 2015. A major source of turbulence in the shelf sea environment is tidal generation (Pingree, 1975), and the lower current velocities in

Table 2
Mean and standard deviation of SCM characteristics and environmental variables during the summer field surveys of 2013, 2014, 2015 and 2016. Nutrient concentrations correspond to the depth of the SCM peak.

	2013	2014	2015	2016
SCM thickness (m)	4.0 ± 3.2	6.3 ± 3.4	4.1 ± 3.1	7.6 ± 6.5
SCM peak chl conc. (μg l^{-1})	3.3 ± 0.8	2.7 ± 0.8	7.3 ± 4.4	3.1 ± 1.8
Top 50 m chl (mg m^{-2})	33.2 ± 9.3	51.9 ± 6.9	42.3 ± 21.5	48.6 ± 12.2
SCM depth (m)	23.0 ± 3.2	26.2 ± 5.0	28.1 ± 2.5	21.7 ± 5.4
SCM temp. (°C)	11.6 ± 0.3	13.1 ± 0.7	12.0 ± 0.2	12.1 ± 0.3
SCM salinity	35.2 ± 0.04	35.2 ± 0.04	35.3 ± 0.01	35.3 ± 0.06
Buoyancy freq. (s^{-1})	0.0025 ± 0.0009	0.0029 ± 0.0012	0.0016 ± 0.0005	0.0036 ± 0.0015
Richardson no.	3.64 ± 2.88	0.42 ± 0.41	9.07 ± 7.83	0.62 ± 0.66
Wind speed (m s^{-1})	4.6 ± 1.9	6.4 ± 3.3	5.6 ± 2.2	6.8 ± 2.3
Current velocity (m s^{-1})	0.25 ± 0.12	0.24 ± 0.09	0.14 ± 0.09	0.28 ± 0.06
Solar insolation (kWh m^{-2} d^{-1})	4.34 ± 1.23	6.49 ± 1.34	5.62 ± 1.68	4.40 ± 1.78
Rainfall (mm d^{-1})	0.9 ± 1.3	2.7 ± 3.3	0.3 ± 0.7	0.2 ± 0.6
Nitrate (μmol l^{-1})	–	0.55 ± 0.20	0.33 ± 0.35	0.39 ± 0.12
Silicate (μmol l^{-1})	–	1.39 ± 0.66	1.14 ± 0.63	0.61 ± 0.16
Phosphate (μmol l^{-1})	–	0.10 ± 0.05	0.15 ± 0.09	0.22 ± 0.05

2015 can be related to tidal phase since the majority of profiles were collected during late spring to mid neap tides when tidal currents would be weakening/weakest. Reduced tidal generated turbulence therefore may account for the greater stability recorded during the 2015 study period.

4.1.2. Influence of temperature

In 2013, in spite of increased stability, peak chlorophyll concentrations within the SCM were relatively low (Fig. 5b) compared to those of 2015, suggesting another environmental factor may have been limiting growth of the phytoplankton community within the SCM. Temperature within the SCM was found to be significantly lower in 2013, on average by 0.4–1.5 °C (Table 2), than in 2014–2016 (Fig. 6d). Given that temperature is a fundamental governing factor of phytoplankton growth and processes required for growth, such as resource attainment (Eppley, 1972; Moisan et al., 2002; Raven and Geider, 1988), the lower temperature in 2013 may have accounted, at least in part, for the relatively low peak SCM chlorophyll concentrations observed. On the other hand, the association between lower temperature and lower peak chlorophyll concentration may simply have been a reflection of the specific physiology, life history and biological interactions of the phytoplankton that were dominating the SCM at the lower temperatures of that year. Temperature within the SCM was significantly higher in 2014, by at least 1 °C on average (Table 2), relative to the other three years. This higher temperature was not accompanied by increased chlorophyll, although it may have influenced phytoplankton community structure (see 4.3 below).

4.2. Environmental controls on SCM phytoplankton community structure assessed by flow cytometry and microscopy

SCM phytoplankton community structure as analysed by flow cytometry was statistically distinct in every year of study (Figs. 7 and 8 and Table 3) according to environmental characteristics (stratification strength, stability and silicate concentration; Supplementary Table 3) specific to each year (Fig. 11). Micro- and meso-phytoplankton were consistently dominant within the SCM when waters were highly stable (Ri mean and standard deviation of 9.07 ± 7.83; Table 2) and silicate concentrations were relatively high (1.14 ± 0.63 μmol l^{-1}; Table 2) as observed in 2015 (Figs. 7 and 11). This association between the dominance of larger (>20 μm) phytoplankton and stability and silicate concentrations largely reflects the physiology of the larger cells.

Community structure of the ≥10 μm phytoplankton within the SCM as identified by light microscopy also varied distinctly over the four years (Figs. 9, 10 and 12 and Table 4) according to the environmental conditions (silicate concentration, temperature, stability, nitrate to phosphate and silicate ratios and phosphate concentration;

Table 3
The top three contributors to similarity within each year based on phytoplankton data compiled using CytoSense flow cytometry (no phytoplankton samples for CytoSense flow cytometry analysis were collected in 2013). Average similarity within each year is also given.

	Top three contributors to similarity (with % contributions)			
	2013	2014	2015	2016
1.	–	Micro- and meso-phytoplankton (40.51)	Micro- and meso-phytoplankton (62.50)	Red nano-phytoplankton (36.69)
2.	–	Red nano-phytoplankton (39.65)	Red nano-phytoplankton (18.97)	Orange pico-phytoplankton (22.76)
3.	–	Orange pico-phytoplankton (10.84)	Orange pico-phytoplankton (9.62)	Micro- and meso- phytoplankton (19.19)
Cumulative contribution (%)	–	91.00	91.09	78.63
Average similarity (%)	–	90.88	89.78	89.37

Table 4
The five greatest contributors to similarity within each year based on phytoplankton data compiled using inverted light microscope analysis. Average similarity within each year is also given.

	Top five contributors to similarity (with % contributions)			
	2013	2014	2015	2016
1.	S *Pseudo-nitzschia spp.* (20.03)	20–25 μm naked dinoflagellates (9.25)	*Tripos fusus* (18.45)	*Chaetoceros* spp. (10.53)
2.	10–20 μm naked dinoflagellates (12.42)	10–20 μm naked dinoflagellates (8.38)	L aloricate ciliates (8.02)	10–20 μm naked dinoflagellates (10.38)
3.	*Tripos lineatus* (10.49)	*Tripos lineatus* (7.97)	10–20 μm naked dinoflagellates (5.24)	L aloricate ciliates (8.79)
4.	*Chaetoceros* spp. (5.97)	*Gyrodinium* spp. (6.60)	*Tripos lineatus* (4.76)	20–25 μm naked dinoflagellates (8.76)
5.	*Diplopsalis lenticula* (5.57)	*Leptocylindrus danicus* (6.46)	*Proboscia truncata* (4.73)	L *Protoperidinium* spp. (5.90)
Cumulative contribution (%)	54.47	38.66	41.21	44.36
Average similarity (%)	70.38	66.87	67.59	69.59

Supplementary Table 3) specific to each year (Fig. 12). While several key taxa occur throughout, each year is characterised by different dominant species (Fig. 9).

Red nano-phytoplankton (such as small naked dinoflagellates, chlorophytes and prymnesiophytes as observed by flow cytometry; details in Table 3) accounted for a greater proportion of the community, often being dominant, in waters with lower stability (Ri $<$ 0.7 on average; Table 2), as observed in 2014 and 2016 (Figs. 7 and 11). The greater instability, frequently resulting in turbulence (Ri $<$ 0.25) was likely unfavourable to the development of a stable niche required by the larger phytoplankton, the diatoms and dinoflagellates of the SCM (Kemp et al., 2000; Kemp and Villareal, 2018). Two key traits that combined may have enabled high contributions and often dominance of nano-phytoplankton within the SCM in low stability conditions, are (1) motility (Kamykowski and McCollum, 1986; Sommer, 1988), facilitating their maintenance and subsequent growth within the SCM, and limiting losses due to turbulent dispersal; and (2) enhanced light utilisation efficiency (Tilstone et al., 1999; Uitz et al., 2008), potentially enabling faster chlorophyll synthesis in the low light conditions of the SCM relative to other phytoplankton, which in turn could act to counterbalance losses to turbulent dispersal. However, low stability conditions were associated with relatively low peak SCM chlorophyll concentrations (Fig. 5b and Table 2), suggesting that turbulent dispersal may have ultimately prevented significant proliferation of the red nano-phytoplankton community at the depth of the SCM. Moreover, as phytoplankton-grazer contact rates are dependent upon turbulence (Lewis et al., 2017; Rothschild and Osborn, 1988) and the main grazers of small phytoplankton have growth rates that are comparable to their prey (Kiørboe, 1993), grazing may also have had a key role in restricting proliferation of the red nano-phytoplankton population.

Also increasing in dominance with increased instability were larger naked dinoflagellates and *Dinophysis* spp. (Figs. 9 and 12) particularly in 2014, with motility, again a likely key favourable trait. Similarly, ciliates were a significant component of the SCM community in 2014–2016 (Fig. 9), but increased ciliate biomass was found when silicate concentrations were higher. Ciliates are typically mixotrophic or heterotrophic and therefore their distribution may often be strongly dependent on specific prey (Löder et al., 2011; Smetacek, 1981). Their association with higher silicate concentrations may reflect a predication for dinoflagellates, flagellates and/or lightly silicified diatoms, such as *Leptocylindrus danicus*.

In 2013, 2014 and 2016 temperature and nutrients (silicate concentration and the Ni:P ratio) emerged as the most important environmental variables governing phytoplankton taxa (Fig. 12), and the SCM community from microscope counts was predominantly a mixed assemblage of diatoms and dinoflagellates (Fig. 9). However, in 2013 and 2016 smaller diatoms (generally $<$400 μm^3 in volume: *Chaetoceros* spp. and *Pseudo-nitzschia* spp.) and smaller dinoflagellates ($<$15000 μm^3 in volume: *Prorocentrum micans* and *Diplopsalis lentiula*) were common (Fig. 9), identified in SCM waters that were relatively cooler (11.6 ± 0.3 and 12.1 ± 0.3 °C in 2013 and 2016 respectively; Table 2), and in the case of 2016, had the lowest silicate concentrations (0.61 ± 0.16 μmol l^{-1}) and Ni:P ratios (1.77 ± 0.32). In contrast, in 2014, common diatoms were larger ($>$1000 μm^3 in volume: large *Rhizosolenia* spp., *Lauderia annulata* and *Leptocylindrus danicus*) and so too were the common dinoflagellates ($>$15000 μm^3 in volume: *Gyrodinium* spp. and *Polykrikos* spp.; Fig. 9). These larger taxa were found in SCM waters that were relatively warmer (13.1 ± 0.7 °C; Table 2), and with the highest recorded silicate concentrations (1.39 ± 0.66 μmol l-1) and Ni:P ratios (6.48 ± 3.71) (Fig. 12). *Diplopsalis lenticula*, *Gyrodinium* spp. and *Polykrikos* spp. are heterotrophic, thus, their occurrence may simply indicate the presence of suitable prey rather than the environmental conditions they were exposed to within the SCM. Small diatoms tend to have higher growth rates (Chisholm, 1992), with *Pseudo-nitzschia* spp. and *Chaetoceros* spp. both characterised by inherently high rates of growth ($>$1 division d^{-1} (Montagnes and Franklin, 2001; Pan et al., 1993)). Given that diatom growth rates tend to follow a linear response with increasing temperature (Montagnes and Franklin, 2001), it is possible that the faster growth rates of these particular small diatoms compensated somewhat for reduced growth related to cooler waters, enabling their significant propagation within the SCM in lieu of larger diatoms, as observed in 2013 and 2016. On the other hand, the warmer waters of 2014 likely favoured increased proportions of larger diatoms (large *Rhizosolenia* spp., *Lauderia annulata* and *Leptocylindrus danicus*) within the SCM due to the positive effects of temperature on growth and subsequent chlorophyll proliferation within the SCM (Eppley, 1972; Moisan et al., 2002; Montagnes and Franklin, 2001; Raven and Geider, 1988). It has been shown for *Leptocylindrus danicus* that cell division rates more than double between 10 and 15 °C (Verity, 1982).

Location of the SCM between 5 and 15 m below the base of the thermocline is evident in several of the CTD profiles in 2016 (Fig. 4b) and is consistent with the low stability values determined for the depth interval of the SCM (Fig. 6a; Supplementary Table 3) as turbulence is largely dissipated at the thermocline boundaries (Sharples et al., 2001). Strong stratification reducing nitrate flux into the thermocline may act to decouple the nitracline from the thermocline (Bjørnsen et al., 1993; Cullen and Eppley, 1981; Holligan et al., 1984c; Karlson et al., 1996; Kononen et al., 2003). As SCM phytoplankton remove available nutrients from within the thermocline, the nitracline deepens, which in turn causes the SCM to deepen (generally in association with the upper nitracline) as phytoplankton respond to utilise nutrients as deep as possible in the nitracline to support growth (Bjørnsen et al., 1993; Sharples et al., 2001). This scenario would favour taxa with motility and the dominant groups within the SCM in 2016 include red nano-phytoplankton and orange pico-phytoplankton (Fig. 7), known to be motile, for example *Synechococcus* can migrate at rates of up to 2 m per day (Ehlers and Oster, 2012). In 2014 there are also a few instances of SCM below the thermocline and these are associated with increased nano- but not pico-phytoplankton. These findings are consistent with those of Karlson et al. (1996), who identified significant populations of $<$3 μm phytoplankton, including pico-eukaryotes and *Synechococcus*, within SCM located 5–10 m below the thermocline in the summer stratified waters of the Skagerrak.

The increased contributions of orange nano-phytoplankton and pico-phytoplankton were also found in SCM waters with reduced silicate (0.61 ± 0.16 μmol l^{-1} in 2016; Figs. 7 and 11 and Table 3). This relationship may reflect silicate accumulation by the orange pico-phytoplankton population (Baines et al., 2012; Ohnemus et al., 2016).

4.3. Dominant taxa of the SCM

In this summary, in addition to the repeat station data, we synthesise also the results of the wider surveys of 2013 as reported in Barnett et al. (2019); 2014 in Supplementary Table 5; 2015 as reported in Barnett et al. (2022); 2016 in Supplementary Table 6 (see Table 1 for summary of all data and availability).

4.3.1. 2013 diatoms: Pseudo-nitzschia spp., Rhizosolenia/Proboscia dinoflagellates: Tripos lineatus

Where diatoms dominated the SCM, *Pseudo-nitzschia spp*. typically made up $>$ 70% of the diatom biomass at the repeat station and at the other sampled Western Channel sites, with the exception being the most seaward, where a *Rhizosolenia/Proboscia* association was dominant (Barnett et al., 2019). *Pseudo-nitzschia* is a cosmopolitan genus regularly found within SCMs in the coastal ocean globally (Trainer et al., 2012), and is annually recurrent in the Western Channel (Downes-Tettmar et al., 2013; Widdicombe et al., 2010). High concentrations of *Pseudo-nitzschia spp.* are especially associated with increased stratification stability and are commonly observed in thin layers such as those typical of the 2013 profiles (Fig. 3a), (Du et al., 2016; McManus et al., 2008; Peterson et al., 2007; Rines et al., 2002; Ryan et al., 2010). The well-formed thermoclines and greater stability in 2013 would therefore

have provided an ideal niche for *Pseudo-nitzschia*. Significantly, *Pseudo-nitzschia* spp. was present in high concentrations in the surface waters and in the deep water below the SCM (Barnett et al., 2019), suggesting that it was equally adapted to blooming in the surface waters. *Rhizosolenia/Proboscia* were also present in the surface waters which may reflect their adaptation for buoyancy regulation (Moore and Villareal, 1996; Woods and Villareal, 2008).

Where dinoflagellates were abundant in the SCM, small naked dinoflagellates and *Tripos lineatus* were the most common. *T. lineatus* is primarily photosynthetic (Rivkin and Voytek, 1985) and is a strong swimmer (Nielsen, 1991). Furthermore, as a relatively large and armoured dinoflagellate, smaller copepods avoid it (Verity and Paffenhofer, 1996). Such characteristics make it well adapted to thrive in the SCM. Unlike for *Pseudo-nitzschia* spp. *T. lineatus* was absent from the surface waters, supporting the assumption of a unique adaptation to the SCM niche.

4.3.2. 2014: dinoflagellates: naked and Tripos lineatus; diatoms: Leptocylindrus danicus

In contrast to 2013 and 2015, no single genus/species was dominant in 2014. Smaller phytoplankton were more significant, primarily red nano-phytoplankton including naked dinoflagellates. Heterotrophic dinoflagellates, primarily *Gyrodinium* and *Polykrikos* were more abundant than in other years contributing around 20% of biomass. Other than heterotrophs the main contributor was *T. lineatus* (as for 2013). In the rarer well-formed SCM, diatoms contributed up to 50% of the biomass, with *Leptocylindrus danicus* as the major contributor with between 67% and 94% of the diatom total biomass. *L. danicus* has been recorded as a major contributor to summer deep chlorophyll maxima in the North-western Mediterranean (Estrada et al., 1993). In general, it appeared that the increased instability at the level of the SCM evidently favoured the increase in smaller, motile phytoplankton, that were better adapted to these conditions than the larger diatoms and dinoflagellates, but that the higher temperatures nevertheless enhanced diatom growth. *T. lineatus* was absent from surface waters while *L.danicus* was rare (Supplementary Table 5).

4.3.3. 2015: dinoflagellate: Tripos fusus

In 2015 the SCM community was overwhelmingly dominated by *Tripos fusus* (Fig. 9), where waters at the depth interval of the SCM were highly stable (Ri of 9.07 ± 7.83; Table 2) (Fig. 12). *T. fusus* was observed to dominate SCMs, not only in the Western Channel but also in the Celtic Sea (Barnett et al., 2022). A prevalence of dinoflagellates has often been observed in more stable waters (Baek et al., 2007b; Cushing, 1989; Pingree et al., 1978), likely because motility enables these phytoplankton to access nutrient rich waters below the thermocline (Baek et al., 2009a; Eppley et al., 1968). In all other years, when stability was typically considerably less, the ≥10 μm phytoplankton community was more of a mixed assemblage of diatoms and generally smaller dinoflagellates (Fig. 9). Traits that may have enabled the dominance of *T. fusus* over other motile phytoplankton include luxury consumption of nutrients (Baek et al., 2008a), mixotrophy, considerable physiological flexibility (Baek et al., 2007b, 2008b; Johns and Reid, 2001), and means of limiting predation pressure, including anoxia (Onoue, 1990; Spatharis et al., 2009) and elongate apical horns (Hamm and Smetacek, 2007; Smetacek, 2001). The dominance of *T. fusus* was also associated with relatively higher/intermediate silicate concentrations (1.14 ± 0.63 μmol l^{-1}; Table 2), and, to a lesser extent, phosphate concentrations (0.15 ± 0.09 μmol l^{-1}) in 2015; (Table 2; Supplementary Table 2) (Fig. 12). This relation to silicate is potentially reflective of the absence of a dominant diatom population at the SCM utilising the silicate supply, and the relation to phosphate may be indicative of the lesser growth dependence of *T. fusus* on phosphate relative to nitrate (Baek et al., 2008a). *T. fusus* was absent from surface waters, again suggesting an adaptation only to the SCM niche. In the less well developed SCM, *Dinophysis* spp. and ciliates were more prominent in 2015.

4.3.4. 2016: mixed: orange pico-phytoplankton; naked dinoflagellates; diatom: Chaetoceros spp

The dominant phytoplankton in the SCM in 2016 constituted the smallest size community in any year with naked dinoflagellates/red nano-phytoplankton and orange pico-phytoplankton the main contributors. Similar to 2014, it appeared that the increased instability and turbulence evident at the SCM favoured the smaller phytoplankton. A further characteristic was the common development of the SCM some 5–15 m below the thermocline. This may indicate that the nutricline was decoupled from the thermocline favouring a smaller motile phytoplankton population. The SCMs were commonly also much thicker than other years. As for 2014, in some of the best-formed SCMs, diatoms made up around 50% of the biomass with *Chaetoceros* spp. contributing 66–99% of the diatom total biomass. *Chaetoceros* spp. has been observed in deep summer blooms in the Northwater (Booth et al., 2002); as a major component of summer deep chlorophyll maxima in the North-western Mediterranean (Estrada et al., 1993), and as a predominant contributor to summer DCM in the NE Atlantic (Latasa et al., 2017). *Chaetoceros* spp. was very rare in the surface waters that were dominated by small (nanoplankton) naked dinoflagellates, heterotrophic dinoflagellates and ciliates where these groups also made up 40–90% of the SCM biomass.

4.3.5. Contrasts in species distributions and adaptations: SCM versus surface water taxa

Taxa that were key components of the SCM phytoplankton in any given year show distinctive distributions with regard to their presence in the rest of the water column. In 2013, *Pseudo-nitzschia* spp., a dominant component of the SCM was equally abundant in the surface and deep waters (Barnett et al., 2019). In fact, *Pseudo-nitzschia* spp., is regularly abundant in summer surface waters monitored at the L4 site (Widdicombe et al., 2010) and accounted for 100% of the diatom community there in August 2009 (Downes-Tettmar et al., 2013), consistent with its documented ubiquity in the coastal ocean (Trainer et al., 2012). By contrast, other diatoms that were significant SCM taxa (*L. danicus* in 2014 and *Chaetoceros* spp. in 2016) were very rare in surface waters. *Chaetoceros* spp. feature as regular spring and summer surface bloom taxa at the L4 (1992–2007) time series (Widdicombe et al., 2010). It therefore appears that these diatom taxa, while a common component of the surface spring and summer blooms are also adapted to shallow SCM that form as stratification develops in the summer. On the other hand, the dinoflagellates *T. lineatus* (significant in the SCM in 2013 and 2014 and present in 2015) and *T. fusus* (dominant in 2015) were not present in surface waters, apparently signifying adaptations uniquely for the SCM niche. These dinoflagellates are both mixotrophs with a range of strategies, as mentioned above, that would allow them to subsist pending intermittent nutrient input including phagotrophy, luxury nutrient uptake and survival in low light (Baek et al., 2007a, 2008b, 2009b). Similarly the *Rhizosolenia/Proboscia* diatoms may be significant components of the SCM but are not observed in surface blooms, in keeping with their adaptation to stratified conditions (Kemp and Villareal, 2018).

4.3.6. Interannual continuity and extent of the SCM community

In the four years monitored, the SCM in the Western English Channel had distinctly different phytoplankton community structure. There was some limited continuity, as demonstrated by the SCM-adapted mixotrophic dinoflagellate, *T. lineatus*, which was significant in 2013 and 2014 and present, albeit in much lower levels in 2015. The distinct year on year differences were developed over a broader area of the Western English Channel extending into the Celtic Sea. A survey of surface (4 m depth) samples from the Western Channel and Celtic Sea noted a change from a microphytoplankton-dominated community in 2013 to a nano-phytoplankton dominated community in 2014 that also had a greater presence of ciliates (Capuzzo et al., 2022). This is a similar pattern to that of the Western Channel SCM. Likewise, in 2015, the dinoflagellate

T. fusus was dominant in the Western Channel SCM and also in SCM sampled in the Celtic Sea (Barnett et al., 2022).

4.3.7. Lack of commonality between SCM and surface spring bloom taxa

To investigate any potential commonality between surface water spring bloom species and summer SCM species the data from the Western Channel Observatory L4 monitoring (10m samples) was inspected for the days of highest phytoplankton abundance in the spring (May–June) interval (Widdicombe and Harbour, 2021). In 2013 and 2014 there was no overlap between the dominant spring bloom taxa and those of the SCM, and in both years *Phaeocystis* was the main L4 taxa. In 2015, *T. fusus* comprised around 25% of the phytoplankton for one day only and was otherwise less than 1% and there was no other overlap. In 2016 there was little evidence of a spring bloom, but with *Phaeocystis* the most important taxa. While there was little evidence of spring bloom/SCM species commonality in the years monitored here, some taxa dominant in the SCM including *Pseudo-nitzschia* spp. (2013) and *Chaetoceros* spp. (2016) have been prominent in the spring bloom monitored at L4 in earlier years (Widdicombe et al., 2010). Consequently, it is likely that the distinct community composition seen at the repeat station presented in our present study result from hydrographic and ecosystem interactions around the time of sampling, rather than strongly connected to potential seed populations remaining from the spring bloom.

5. Conclusions

Repeat sampling of the summer (late June to early July) stratified waters of the Western English Channel over the years 2013–2016, reveals interannual variability in environmental conditions, SCM chlorophyll structure and phytoplankton communities.

High water column stability at the depth of the SCM, as evidenced by large Richardson numbers and a well-developed strong thermocline, favoured the growth of larger dinoflagellates (autotrophs or mixotrophs) and diatoms. Such conditions led to development of the most intense SCMs and these were sometimes dominated by a single or a few key species including the dinoflagellates *Tripos fusus* and *Tripos lineatus*, and the diatoms *Leptocylindricus danicus* and *Rhizosolenia/Proboscia*. Most notably, in 2015, up to 85% of the SCM phytoplankton biomass comprised the dinoflagellate *T. fusus*, coinciding with the most stable conditions observed over the 4 years. In 2015 *T. fusus* was also dominant in SCMs in the Celtic Sea evidencing the widespread dispersal of key species. The highest peak SCM chlorophyll concentrations were also observed in 2015 (7.3 ± 4.4 μg l^{-1}) in association with greater stability at the depth interval of the SCM (Ri of 9.07 ± 7.83), which was related to significantly lower current velocities (0.14 ± 0.09 m s^{-1}). There did not appear to be continuity of key species between years, other than for the dinoflagellate *T. lineatus*, which was significant in both 2013 and 2014 and present in 2015.

Low water column stability and intermittent turbulence (low Ri) in 2014 and 2016 led to greater chlorophyll dispersal in the water column relative to 2013 and 2015 particularly below the SCM. Red fluorescent nano-phytoplankton, such as naked dinoflagellates, chlorophytes and prymnesiophytes, made a greater contribution to the community, possibly as a result of the advantages that motility and enhanced light utilisation efficiency confer within an SCM exposed to turbulence. It is also likely that turbulence disrupted the stability required by the larger dinoflagellates and diatoms. Orange fluorescent nano-phytoplankton and pico-phytoplankton, such as cryptophytes, *Synechococcus*, chlorophytes and prymnesiophytes, were also more important in the SCM community when the SCM was 5–15 m deeper than the thermocline.

Several of the key SCM taxa were absent from surface waters including the dinoflagellates *T. fusus*, *T. lineatus*, and most of the *Rhizosolenia/Proboscia* diatoms, consistent with adaptations more suited to survival at depth in stratified waters. These traits include luxury nutrient uptake and storage and survival in low light (both groups) and mixotrophy (dinoflagellates only). On the other hand, on separate occasions, diatoms including *Pseudo-nitszchia* spp. were abundant in both surface, SCM and bottom waters. In any given year, there was no correspondence between the key spring bloom phytoplankton species as monitored in the nearby Western Channel Observatory L4 station and the key SCM taxa.

A further key relationship was that of SCM temperature, with cooler waters (11.6–12.1 °C on average) in 2013 and 2016 favouring smaller diatoms (*Chaetoceros* spp. and *Pseudo-nitzschia* spp.), and slightly warmer waters (13.1 °C on average) in 2014 favouring larger diatoms (large *Rhizosolenia* spp., *Lauderia annulata* and *Leptocylindrus danicus*). This relationship between temperature and size may be significant for carbon export to depth, and for the occurrence of toxic species (*Pseudo-nitzschia* spp.).

CRediT authorship contribution statement

Michelle L. Barnett: Writing – review & editing, Writing – original draft, Software, Methodology, Investigation, Formal analysis, Data curation, Conceptualization. **Alan E.S. Kemp:** Writing – review & editing, Supervision, Project administration, Investigation, Formal analysis, Conceptualization. **Anna E. Hickman:** Writing – review & editing, Supervision, Methodology, Investigation, Funding acquisition, Conceptualization. **Duncan A. Purdie:** Writing – review & editing, Supervision, Project administration, Methodology, Investigation, Funding acquisition, Conceptualization.

Declaration of competing interest

The authors declare that they have no known competing financial interests or personal relationships that could have appeared to influence the work reported in this paper.

Data availability

Data will be made available on request.

Acknowledgements

We thank Bill Fletcher, Gary Fisher and Nick Hazeldine (University of Southampton) for crewing the vessel RV Callista that allowed us to conduct this research. This research was funded by a University of Southampton Graduate School of the National Oceanography Centre Southampton (GSNOCS) Ph.D. studentship to Michelle Barnett, with additional support from the Natural Environment Research Council (UK) "CaNDyFloSS: Carbon and Nutrient Dynamics and Fluxes over Shelf Systems" grant NE/K00185X/1 to AEH and DAP.

Appendix A. Supplementary data

Supplementary data to this article can be found online at https://doi.org/10.1016/j.csr.2024.105253.

References

Backhaus, J.O., 1996. Climate-sensitivity of European marginal seas, derived from the interpretation of modelling studies. J. Mar. Syst. 7, 361–382.
Baek, S.H., Shimode, S., Han, M.S., Kikuchi, T., 2008a. Growth of dinoflagellates, *Ceratium furca* and *Ceratium fusus* in Sagami Bay, Japan: the role of nutrients. Harmful Algae 7, 729–739.
Baek, S.H., Shimode, S., Kikuchi, T., 2007a. Reproductive ecology of the dominant dinoflagellate, *Ceratium fusus*, in coastal area of Sagami Bay, Japan. J. Oceanogr. 63, 35–45.
Baek, S.H., Shimode, S., Kikuchi, T., 2007b. Reproductive ecology of the dominant dinoflagellate, *Ceratium fusus*, in coastal area of Sagami Bay, Japan. J. Oceanogr. 63, 35–45.
Baek, S.H., Shimode, S., Kikuchi, T., 2008b. Growth of dinoflagellates, *Ceratium furca* and *Ceratium fusus* in Sagami Bay, Japan: the role of temperature, light intensity and photoperiod. Harmful Algae 7, 163–173.

Baek, S.H., Shimode, S., Shin, K., Han, M.-S., Kikuchi, T., 2009a. Growth of dinoflagellates, *Ceratium furca* and *Ceratium fusus* in Sagami Bay, Japan: the role of vertical migration and cell division. Harmful Algae 8, 843–856.
Baek, S.H., Shimode, S., Shin, K., Han, M.S., Kikuchi, T., 2009b. Growth of dinoflagellates, *Ceratium furca* and *Ceratium fusus* in Sagami Bay, Japan: the role of vertical migration and cell division. Harmful Algae 8, 843–856.
Baines, S.B., Twining, B.S., Brzezinski, M.A., Krause, J.W., Vogt, S., Assael, D., McDaniel, H., 2012. Significant silicon accumulation by marine picocyanobacteria. Nature Geoscience Letters 5, 886–891.
Barnes, M.K., Tilstone, G.H., Suggett, D.J., Widdicombe, C.E., Bruun, J., Martinez-Vicente, V., Smyth, T.J., 2015. Temporal variability in total, micro- and nano-phytoplankton primary production at a coastal site in the Western English Channel. Prog. Oceanogr. 137, 470–483.
Barnett, M.L., Kemp, A.E.S., Hickman, A.E., Purdie, D.A., 2019. Shelf sea subsurface chlorophyll maximum thin layers have a distinct phytoplankton community structure. Continent. Shelf Res. 174, 140–157.
Barnett, M.L., Kemp, A.E.S., Nimmo-Smith, W.A.M., Purdie, D.A., 2022. Total water column analysis shows the importance of a single species in subsurface chlorophyll maximum thin layers in stratified waters. Front. Mar. Sci. 8.
Barton, A.D., Taboada, F.G., Atkinson, A., Widdicombe, C.E., Stock, C.A., 2020. Integration of temporal environmental variation by the marine plankton community. Mar. Ecol. Prog. Ser. 647, 1–16.
Beaugrand, G., Ibanez, F., Reid, P.C., 2000. Spatial, seasonal and long-term fluctuations of plankton in relation to hydroclimatic features in the English Channel, Celtic Sea and Bay of Biscay. Mar. Ecol. Prog. Ser. 200, 93–102.
Beaugrand, G., Reid, P.C., 2003. Long-term changes in phytoplankton, zooplankton and salmon related to climate. Global Change Biol. 9, 801–817.
Benoit-Bird, K.J., McManus, M.A., 2012. Bottom-up regulation of a pelagic community through spatial aggregations. Biol. Lett. 8, 813–816.
Bjørnsen, P.K., Kaas, H., Kaas, H., Nielsen, T.G., Olesen, M., Richardson, K., 1993. Dynamics of a subsurface phytoplankton maximum in the Skagerrak. Mar. Ecol. Prog. Ser. 95, 279–294.
Booth, B.C., Larouche, P., Belanger, S., Klein, B., Amiel, D., Mei, Z.P., 2002. Dynamics of *Chaetoceros socialis* blooms in the North water. Deep-Sea Res Pt Ii 49, 5003–5025.
Bray, N.A., Fofonoff, N.P., 1981. Available potential energy for MODE eddies. J. Phys. Oceanogr. 11, 30–46.
Capuzzo, E., Wright, S., Bouch, P., Collingridge, K., Creach, V., Pitois, S., Stephens, D., Van der Kooij, J., 2022. Variability in structure and carbon content of plankton communities in autumn in the waters south-west of the UK. Prog. Oceanogr. 204.
Chisholm, S.W., 1992. Phytoplankton size. In: Falkowski, P.G., Woodheaf, A.D. (Eds.), Primary Productivity and Biogeochemical Cycles in the Sea. Plenum. Springer, USA, pp. 213–237.
Clarke, K.R., Gorley, R.N., 2006. PRIMER V6: User Manual/Tutorial. PRIMER-E, Plymouth.
Clarke, K.R., Warwick, R.M., 2001. Change in Marine Communities: an Approach to Statistical Analysis and Interpretation, second ed. PRIMER-E, Plymouth.
Cullen, J.J., 1982. The deep chlorophyll maximum - comparing vertical profiles of chlorophyll-a. Can. J. Fish. Aquat. Sci. 39, 791–803.
Cullen, J.J., 2015. Subsurface chlorophyll maximum layers: enduring enigma or mystery solved? Ann. Rev. Mar. Sci 7, 207–239.
Cullen, J.J., Eppley, R.W., 1981. Chlorophyll maximum layers of the Southern California Bight and possible mechanisms of their formation and maintenance. Oceanol. Acta 4, 23–32.
Cushing, D.H., 1989. A difference in structure between ecosystems in strongly stratified waters and in those that are only weakly stratified. J. Plankton Res. 11, 1–13.
Dauvin, J.-C., 2012. Are the eastern and western basins of the English Channel two separate ecosystems? Mar. Pollut. Bull. 64, 463–471.
Downes-Tettmar, N., Rowland, S., Widdicombe, C., Woodward, M., Llewellyn, C., 2013. Seasonal variation in Pseudo-nitzschia spp. and domoic acid in the western English channel. Continent. Shelf Res. 53, 40–49.
Du, X., Peterson, W., Fisher, J., Hunter, M., Peterson, J., 2016. Initiation and development of a toxic and persistent *Pseudo-nitzschia* bloom off the Oregon coast in spring/summer 2015. PLoS One 11. https://doi.org/10.1371/journal.pone.0163977.
Ehlers, K., Oster, G., 2012. On the Mysterious Propulsion of Synechococcus. PLoS One 7.
Eppley, R.W., 1972. Temperature and phytoplankton growth in the sea. Fish. Bull. 70, 1063–1085.
Eppley, R.W., Holm-Harisen, O., Strickland, J.D.H., 1968. Some observations of the vertical migration of dinoflagellates. J. Phycol. 4, 333–340.
Estrada, M., Marrase, C., Latasa, M., Berdalet, E., Delgado, M., Riera, T., 1993. Variability of deep chlorophyll maximum characteristics in the Northwestern Mediterranean. Mar. Ecol. Prog. Ser. 92, 289–300.
Fernand, l., Weston, K., Morris, T., Greenwood, N., Brown, J., Jickells, T., 2013. The contribution of the deep chlorophyll maximum to primary production in a seasonally stratified shelf sea, the North Sea. Biogeochemistry 113, 153–166.
Fishwick, J.R., 2017. CTD Profiles (Depth, Pressure, Temperature, Salinity, Potential Temperature, Density, Fluorescence, Transmissance, Downwelling PAR, Dissolved Oxygen Concentration) Binned to 0.5 M and 0.25 M at Sites L4 and E1 in the Western English Channel between January 2002 and December 2016. British Oceanographic Data Centre - Natural Environment Research Council, UK.
Goldman, J.C., 1993. Potential role of large oceanic diatoms in new primary production. Deep-Sea Res. 40, 159–168.
Graff, J.R., Rynearson, T.A., 2011. Extraction method influences the recovery of phytoplankton pigments from natural assemblages. Limnol Oceanogr. Methods 9, 129–139.
Grasshoff, K., 1976. Methods of Seawater Analysis. Verlag Chemie, Weinheim, Germany.
Hamm, C., Smetacek, V., 2007. Armor: Why, when, how. In: Falkowski, P.G., Knoll, A.H. (Eds.), Evolution of Primary Producers in the Sea. Elsevier, Burlington, USA, pp. 311–332.
Heath, M.R., Beare, D.J., 2008. New primary production in northwest European shelf seas, 1960-2003. Mar. Ecol. Prog. Ser. 363, 183–203.
Hickman, A.E., Moore, C.M., Sharples, J., Lucas, M.I., Tilstone, G.H., Krivtsov, V., Holligan, P.M., 2012. Primary production and nitrate uptake within the seasonal thermocline of a stratified shelf sea. Mar. Ecol. Prog. Ser. 463, 39–57.
Holligan, P.M., Balch, W.M., Yentsch, C.M., 1984a. The significance of subsurface chlorophyll, nitrite and ammonium maxima in relation to nitrogen for phytoplankton growth in stratified waters of the Gulf of Maine. J. Mar. Res. 42, 1051–1073.
Holligan, P.M., Harbour, D.S., 1977. The vertical distribution and succession of phytoplankton in the western English channel in 1975 and 1976. Journal of the Marine Biological Association of the UK 57, 1075–1093.
Holligan, P.M., Harris, R.P., Newell, R.C., Harbour, D.S., Head, R.N., Linley, E.A.S., Lucas, M.I., Tranter, P.R.G., Weekley, C.M., 1984b. Vertical distribution and partitioning of organic carbon in mixed, frontal and stratified waters of the English Channel. Mar. Ecol. Prog. Ser. 14, 111–127.
Holligan, P.M., Williams, P.J.L., Purdie, D., Harris, R.P., 1984c. Photosynthesis, respiration and nitrogen supply of plankton populations in stratified, frontal and tidally mixed shelf waters. Mar. Ecol. Prog. Ser. 17, 201–213.
Holt, J., Schrum, C., Cannaby, H., Daewel, U., Allen, I., Artioli, Y., Bopp, L., Butenschon, M., Fach, B.A., Harle, J., Pushpadas, D., Salihoglu, B., Wakelin, S., 2016. Potential impacts of climate change on the primary production of regional seas: a comparative analysis of five European seas. Prog. Oceanogr. 140, 91–115.
Holt, J., Wakelin, S., Lowe, J., Tinker, J., 2010. The potential impacts of climate change on the hydrography of the northwest European continental shelf. Prog. Oceanogr. 86, 361–379.
Jahnke, R.A., 2010. Global synthesis. In: Liu, K.K., Atkinson, L., Quinones, R.A., Talaue-McManus, L. (Eds.), Carbon and Nutrient Fluxes in Continental Margins: A Global Synthesis. Springer, Berlin.
Jeffrey, S.W., Vesk, M., 1997. Introduction to marine phytoplankton and their pigment signatures. In: Jeffrey, S.W., Mantoura, R.F., Wright, S.W. (Eds.), Phytoplankton Pigments in Oceanography: Guidelines to Modern Methods. UNESCO Publishing, Paris, pp. 37–84.
Johns, D.G., Reid, P.C., 2001. Technical report TR_005: an overview of plankton ecology in the North Sea. Strategic Environmental Assessment - SEA2. SAHFOS, Plymouth, UK.
Kamykowski, D., McCollum, S.A., 1986. The temperature acclimatised swimming speed of selected marine dinoflagellates. J. Plankton Res. 8, 275–287.
Karlson, B., Edler, L., Granéli, W., Sahlsten, E., Kuylenstierna, M., 1996. Subsurface chlorophyll maxima in the Skagerrak - processes and phytoplankton community structure. J. Sea Res. 35, 139–158.
Kemp, A.E.S., Pike, J., Pearce, R.B., Lange, C.B., 2000. The "Fall dump" - a new perspective on the role of a "shade flora" in the annual cycle of diatom production and export flux. Deep-Sea Res. Part II Top. Stud. Oceanogr. 47, 2129–2154.
Kemp, A.E.S., Villareal, T.A., 2013. High diatom production and export in stratified waters – a potential negative feedback to global warming. Prog. Oceanogr. 119, 4–23.
Kemp, A.E.S., Villareal, T.A., 2018. The case of the diatoms and the muddled mandalas: time to recognize diatom adaptations to stratified waters. Prog. Oceanogr. 167, 138–149.
Kiørboe, T., 1993. Turbulence, phytoplankton cell size and the structure of pelagic food webs. Adv. Mar. Biol. 29, 1–61.
Kirkwood, D., 1996. Nutrients: Practical Notes on Their Determination in Seawater, ICES Techniques in Marine Environmental Sciences No.17. ICES, Copenhagen, Denmark.
Kitidis, V., Hardman-Mountford, N.J., Litt, E., Brown, I., Cummings, D., Hartman, S., Hydes, D., Fishwick, J.R., Harris, C., Martinez-Vicente, V., Woodward, E.M.S., Smyth, T.J., 2012. Seasonal dynamics of the carbonate system in the Western English Channel. Continent. Shelf Res. 42, 30–40.
Kononen, K., Huttunen, M., Hällfors, S., Gentien, P., Lunven, M., Huttula, T., Laanemets, J., Lilover, M., Pavelson, J., Stips, A., 2003. Development of a deep chlorophyll maximum of *Heterocapsa triquetra* Ehrenb. at the entrance of the Gulf of Finland. Limnol. Oceanogr. 48, 594–607.
Latasa, M., Cabello, A.M., Moran, X.A.G., Massana, R., Scharek, R., 2017. Distribution of phytoplankton groups within the deep chlorophyll maximum. Limnol. Oceanogr. 62, 665–685.
Lepš, J., Šmilauer, P., 2003. Multivariate Analysis of Ecological Data Using CANOCO. Cambridge University Press, USA.
Lewis, D.M., Brereton, A., Siddons, J.T., 2017. A large eddy simulation study of the formation of deep chlorophyll/biological maxima in un-stratified mixed layers: the roles of turbulent mixing and predation pressure. Limnol. Oceanogr. https://doi.org/10.1002/lno.10566.
Lips, U., Lips, I., Liblik, T., Kuvaldina, N., 2010. Processes responsible for the formation and maintenance of sub-surface chlorophyll maxima in the Gulf of Finland. Estuar. Coast Shelf Sci. 88, 339–349.
Löder, M.G.J., Meunier, C., Wiltshire, K., Aberle, N., 2011. The role of ciliates, heterotrophic dinoflagellates and copepods in structuring spring plankton communities at Helgoland Roads, North Sea. Marine Biology 158, 1551–1580.
Martin, J., Dumont, D., Tremblay, J.-E., 2013. Contribution of subsurface chlorophyll maxima to primary production in the coastal Beaufort Sea (Canadian Arctic: a model assessment. J. Geophys. Res.: Oceans 118, 5873–5886.
Martin, J., Tremblay, J.E., Gagnon, J., Tremblay, G., Lapoussiere, A., Jose, C., Poulin, M., Gosselin, M., Gratton, Y., Michel, C., 2010. Prevalence, structure and properties of

subsurface chlorophyll maxima in Canadian Arctic waters. Mar. Ecol. Prog. Ser. 412, 69–84.
MCCIP, 2008. Marine climate changes impacts annual report card 2007 - 2008. In: Baxter, J.M., Buckley, P.J., Wallace, C.J. (Eds.), MCCIP, Lowestoft, p. 8.
McManus, M.A., Kudela, R.M., Silver, M.W., Steward, G.F., Donaghay, P.L., Sullivan, J. M., 2008. Cryptic blooms: are thin layers the missing connection? Estuar. Coast 31, 396–401.
Menden-Deuer, S., Lessard, E.J., 2000. Carbon to volume relationships for dinoflagellates, diatoms, and other protist plankton. Limnol. Oceanogr. 45, 569–579.
Miles, J., 1961. On the stability of heterogeneous shear flows. J. Fluid Mech. 10, 496–508.
Moisan, J.R., Moisan, T.A., Abbot, M.R., 2002. Modelling the effect of temperature on the maximum growth rates of phytoplankton populations. Ecol. Model. 153, 197–215.
Montagnes, D.J.S., Franklin, D.J., 2001. Effect of temperature on diatom volume, growth rate, and carbon and nitrogen content: reconsidering some paradigms. Limnol. Oceanogr. 46, 2008–2018.
Moore, J.K., Villareal, T.A., 1996. Buoyancy and growth characteristics of three positively buoyant marine diatoms. Mar. Ecol. Prog. Ser. 132, 203–213.
NASA, 2018. Daily Solar Insolation at 50° 05.670 N, 004° 52.020 W for June/July 2013 - 2016 Taken from CERES Fast Longwave and SHortwave Radiative Fluxes (FLASHFlux) Project. NASA.
Nielsen, T.G., 1991. Contribution of zooplankton grazing to the decline of a Ceratium bloom. Limnol. Oceanogr. 36, 1091–1106.
NIOZ, 2015a. QuAAtro Applications Method No. Q-064-05 Rev. 8: Phosphate in Water and Seawater. Nederlands Instituut for Onderzoek der Zee (Royal Netherlands Institute for Sea Research), Den Hoorn (Texel), The Netherlands.
NIOZ, 2015b. QuAAtro Applications Method No. Q-066-05 Rev.5: Silicate in Water and Seawater. Nederlands Instituut for Onderzoek der Zee (Royal Netherlands Institute for Sea Research), Den Hoorn (Texel), The Netherlands.
NIOZ, 2016. QuAAtro Applications Method No. Q-068-05 Rev. 11: Nitrate and Nitrite in Water and Seawater. Nederlands Instituut for Onderzoek der Zee (Royal Netherlands Institute for Sea Research), Den Hoorn (Texel), The Netherlands.
Ohnemus, D.C., Rauschenberg, S., Krause, J.W., Brzezinski, M.A., Collier, J.L., Geraci-Yee, S., Baines, S.B., Twining, B.S., 2016. Silicon content of individual cells of *Synechococcus* from the North Atlantic ocean. Mar. Chem. 187, 16–24.
Olenina, I., Hajdu, S., Edler, L., Andersson, A., Wasmund, N., Busch, S., Göbel, J., Gromisz, S., Huseby, S., Huttunen, M., Jaanus, A., Kokkonen, P., Ledaine, I., Niemkiewicz, E., 2006. Biovolumes and size-classes of phytoplankton in the Baltic sea. HELCOM Baltic Sea Environment Proceedings No. 106, 1–144.
Onoue, Y., 1990. Massive fish kills by a *Ceratium fusus* red tide in Kagoshima Bay, Japan. Red Tide Newsletter 3, 2.
Paasche, E., 1960. On the Relationship between primary production and standing stock of phytoplankton. J. Internat. Counc. Explor. Sea 26, 33–48.
Pan, Y., Subba Rao, D.V., Mann, K.H., Li, W.K.W., Warnock, R.E., 1993. Temperature dependence of growth and carbon assimilation in *Nitzschia pungens f. multiseries*, the causative diatom of domoic acid poisoning. In: Smayda, T.J., Shimizu, Y. (Eds.), Toxic Phytoplankton Blooms in the Sea. Elsevier, New York, pp. 619–624.
Pauly, D., Christensen, V., Guenette, S., Pitcher, T.J., Sumaila, U.R., Walters, C.J., Watson, R., Zeller, D., 2002. Towards sustainability in world fisheries. Nature 418, 689–695.
Peterson, T.D., Toews, H.N.J., Robinson, C.L.K., Harrison, P.J., 2007. Nutrient and phytoplankton dynamics in the Queen Charlotte Islands (Canada) during the summer upwelling seasons of 2001 - 2002. J. Plankton Res. 29, 219–239.
Pingree, R.D., 1975. The advance and retreat of the thermocline on the continental shelf. Journal of the Marine Biological Association of the UK 55, 965–974.
Pingree, R.D., 1980. Chapter 13: Physical Oceanography of the Celtic Sea and English Channel, vol. 24. Elsevier Oceanography Series, pp. 415–465.
Pingree, R.D., Holligan, P.M., Mardell, G.T., 1978. The effects of vertical stability on phytoplankton distribution in the summer on the northwest European shelf. Deep-Sea Res. 25, 1011–1028.
PML, 2017. L4 Autonomous Buoy AirMar Data for the Western English Channel during June/July 2013-2016. NERC.
Raven, J.A., Geider, R.J., 1988. Temperature and algal growth. New Phytol. 110, 441–461.
Richardson, K., Nielsen, T.G., Pedersen, F.B., Heilmann, J.P., Lokkegaard, B., Kaas, H., 1998. Spatial heterogeneity in the structure of the planktonic food web in the North Sea. Mar. Ecol. Prog. Ser. 168, 197–211.
Richardson, K., Visser, A.W., Pedersen, F.B., 2000. Subsurface phytoplankton blooms fuel pelagic production in the North Sea. J. Plankton Res. 22, 1663–1671.
Rines, J.E.B., Donaghay, P.L., Dekshenieks, M.M., Sullivan, J.M., Twardowski, M.S., 2002. Thin layers and camouflage: Hidden *Pseudo-nitzschia* populations in a fjord in the san Juan Islands, Washington, USA. Mar. Ecol. Prog. Ser. 225, 123–137.
Rivkin, R.B., Voytek, M.A., 1985. Photoadaptations of photosynthesis by dinoflagellates from natural populations: a species approach. In: Anderson, D.M., White, A.W., Baden, D.G. (Eds.), Toxic Dinoflagellates. Elsevier, Amsterdam, pp. 97–102.
Rothschild, B.J., Osborn, T.R., 1988. Small-scale turbulence and plankton contact rates. J. Plankton Res. 10, 465–474.
Ryan, J.P., McManus, M.A., Sullivan, J.M., 2010. Interacting physical, chemical and biological forcing of phytoplankton thin-layer variability in Monterey Bay, California. Continent. Shelf Res. 30, 7–16.
Scott, B.E., Sharples, J., Ross, O.N., Wang, J., Pierce, G.J., Camphuysen, C.J., 2010. Sub-surface hotspots in shallow seas: fine-scale limited locations of top predator foraging habitat indicated by tidal mixing and sub-surface chlorophyll. Mar. Ecol. Prog. Ser. 408, 207–226.
Sharples, J., Moore, C.M., Rippeth, T.P., Holligan, P.M., Hydes, D.J., Fisher, N.R., Simpson, J.H., 2001. Phytoplankton distribution and survival in the thermocline. Limnol. Oceanogr. 46, 486–496.
Sharples, J., Ross, O.N., Scott, B.E., Greenstreet, S.P.R., Fraser, H., 2006. Inter-annual variability in the timing of stratification and the spring bloom in the North-western North Sea. Continent. Shelf Res. 26, 733–751.
Sharples, J., Simpson, J.H., 2012. Introduction to the Physical and Biological Oceanography of Shelf Seas. Cambridge University Press, Cambridge.
Smetacek, V., 1981. The annual cycle of protozooplankton in Kiel Bight. Marine Biology 63, 1–11.
Smetacek, V., 2001. A watery arms race. Nature 411, 745, 745.
Smyth, T., 2017. Meteorological Data (Solar Irradiance and Rainfall) Logged by the Omni Instruments 6" Tipping Bucket Raingauge (RG200) and Li-Cor Pyranometer (LI-200SZ) of the PML Meteorological Station between 2013 and 2016. NERC.
Smyth, T.J., Fishwick, J.R., Al-Moosawi, L., Cummings, D.G., Harris, C., Kitidis, V., Rees, A., Martinez-Vicente, V., Woodward, E.M.S., 2010. A broad spatio-temporal view of the Western English Channel observatory. J. Plankton Res. 32, 585–601.
Sommer, U., 1988. Some size relationships in phytoflagellate motility. Hydrobiologia 161, 125–131.
Southward, A.J., Langmead, O., Hardman-Mountford, N.J., Aiken, J., Boalch, G.T., Dando, P.R., Genner, M.J., Joint, I., Kendall, M.A., Halliday, N.C., Harris, R.P., Leaper, R., Mieszkowska, N., Pingree, R.D., Richardson, A.J., Sims, D.W., Smith, T., Walne, A.W., Hawkins, S.J., 2005a. Long-term oceanographic and ecological research in the Western English Channel. In: Southward, A.J., Tyler, P.A., Young, C. M., Fuiman, L.A. (Eds.), Advance in Marine Biology. Elsevier Academic Press, San Diego, USA, pp. 1–105.
Southward, A.J., Langmead, O., Hardman-Mountford, N.J., Aiken, J., Boalch, G.T., Dando, P.R., Genner, M.J., Joint, I., Kendall, M.A., Halliday, N.C., Harris, R.P., Leaper, R., Mieszkowska, N., Pingree, R.D., Richardson, A.J., Sims, D.W., Smith, T., Walne, A.W., Hawkins, S.J., 2005b. A review of long-term research in the western English Channel. In: Southward, A.J., Tyler, P.A., Young, C.M., Fuiman, L.A. (Eds.), Advances in Marine Biology. Elsevier Academic Press, San Diego, USA, pp. 3–84.
Spatharis, S., Dolapsakis, N.P., Economou-Amilli, A., Tsirtsis, G., Danielidis, D.B., 2009. Dynamics of potentially harmful microalgae in a confined Mediterranean Gulf—Assessing the risk of bloom formation. Harmful Algae 8, 736–743.
Stinchcombe, M., 2017. Nitrate, phosphate and silicate detection limits of a SEAL Analytical QuAAtro segmented flow AutoAnalyser. In: Barnett, M. (Ed.), National Oceanography Centre. Southampton.
Sullivan, J.M., Donaghay, P.L., Rines, J.E.B., 2010. Coastal thin layer dynamics: consequences to biology and optics. Continent. Shelf Res. 30, 50–65.
Tarran, G.A., Bruun, J.T., 2015. Nanoplankton and picoplankton in the Western English Channel: abundance and seasonality from 2007-2013. Prog. Oceanogr. 137, 446–455.
ter Braak, C.J.F., Šmilauer, P., 2002. CANOCO Reference Manual and CanoDraw for Windows User's Guide: Software for Canonical Community Ordination (Version 4.5). Microcomputer Power, Ithaca, New York.
Tilstone, G.H., Figueiras, F.G., Fermin, E.G., Arbones, B., 1999. Significance of nanophytoplankton photosynthesis and primary production in a coastal upwelling system (Ria de Vigo, NW Spain). Mar. Ecol. Prog. Ser. 183, 13–27.
Trainer, V.L., Bates, S.S., Lundholm, N., Thessen, A.E., Cochlan, W.P., Adams, N.G., Trick, C.G., 2012. Pseudo-nitzschia physiological ecology, phylogeny, toxicity, monitoring and impacts on ecosystem health. Harmful Algae 14, 271–300.
Uitz, J., Huot, Y., Bruyant, F., Babin, M., Claustre, H., 2008. Relating phytoplankton photophysiological properties to community structure on large scales. Limnol. Oceanogr. 53, 614–630.
Utermöhl, H., 1958. Improvement of the quantitative methods for phytoplankton. International Association of Theoretical and Applied Limnology 9, 1–38.
Verity, P.G., 1982. Effects of temperature, irradiance, and daylength on the marine diatom *Leptocylindrus danicus* cleve .4. Growth. J. Exp. Mar. Biol. Ecol. 60, 209–222.
Verity, P.G., Paffenhofer, G.A., 1996. On assessment of prey ingestion by copepods. J. Plankton Res. 18, 1767–1779.
Welschmeyer, N.A., 1994. Fluorometric analysis of chlorophyll a in the presence of chlorophyll b and pheopigments. Limnol. Oceanogr. 39, 1985–1992.
Weston, K., Fernand, L., Mills, D.K., Delahunty, R., Brown, J., 2005. Primary production in the deep chlorophyll maximum of the central North Sea. J. Plankton Res. 27, 909–922.
Widdicombe, C.E., Eloire, D., Harbour, D., Harris, R.P., Somerfield, P.J., 2010. Long-term phytoplankton community dynamics in the Western English Channel. J. Plankton Res. 32, 643–655.
Widdicombe, C.E., Harbour, D., 2021. Phytoplankton Taxonomic Abundance and Biomass Time-Series at Plymouth Station L4 in the Western English Channel, 1992-2020. NERC EDS British Oceanographic Data Centre NOC, 10/grks.
Williams, C., Sharples, J., Green, M., Mahaffey, C., Rippeth, T., 2013. The maintenance of the subsurface chlorophyll maximum in the stratified western Irish Sea. Limnol. Oceanogr. Fluid. Environ. 3, 61–73.
Wollast, R., 1998. Evaluation and comparison of the global carbon cycle in the coastal zone and in the open ocean. In: Brink, K.H., Robinson, A.R. (Eds.), The Sea. John Wiley and Sons, pp. 213–252.
Woods, S., Villareal, T.A., 2008. Intracellular ion concentrations and cell sap density in positively buoyant oceanic phytoplankton. Nova Hedwigia 131–145.
Xie, Y.Y., Tilstone, G.H., Widdicombe, C., Woodward, E.M.S., Harris, C., Barnes, M.K., 2015. Effect of increases in temperature and nutrients on phytoplankton community structure and photosynthesis in the western English Channel. Mar. Ecol. Prog. Ser. 519, 61–73.
Zuur, A.F., Ieno, E.N., Smith, G.M., 2007. Analysing Ecological Data. Springer, New York.